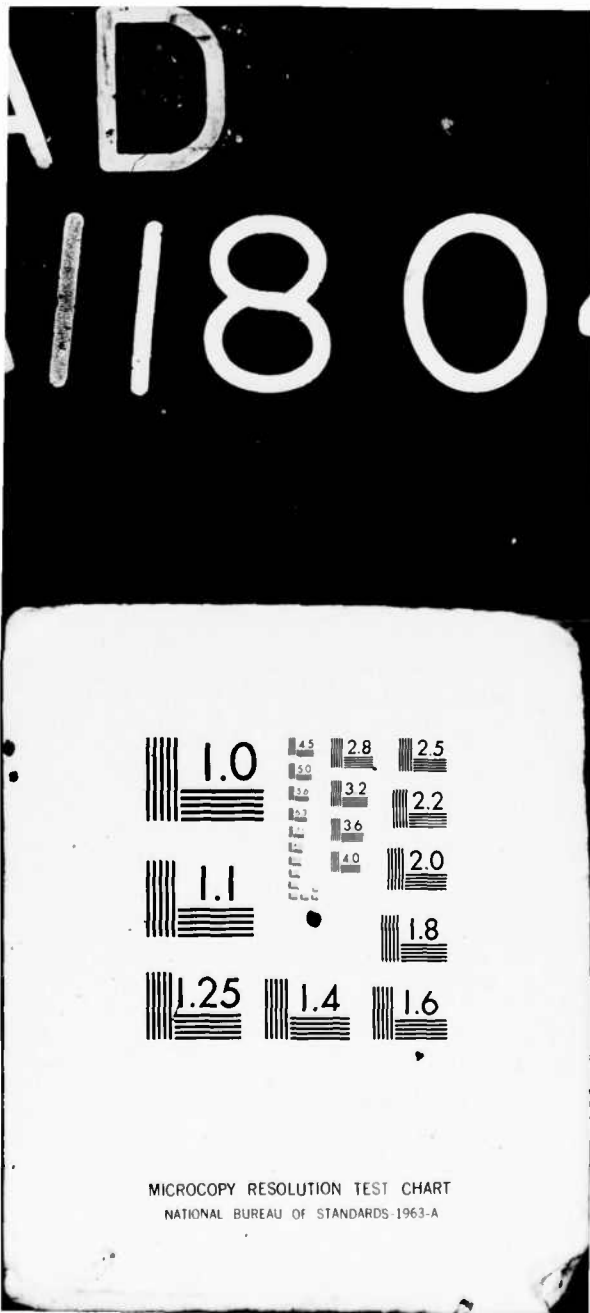


AD-A118 041 AIR FORCE INST OF TECH WRIGHT-PATTERSON AFB OH SCH00--ETC F/6 20/6
MODE ANALYSIS IN A MISALIGNED UNSTABLE RESONATOR.(U)
UNCLASSIFIED DEC 81 R W BERDINE
AFIT/GEP/PH/81D-2 NL

1 OF
AO
A118 041



END
DATE
FILMED
DTIC



MICROCOPY RESOLUTION TEST CHART
NATIONAL BUREAU OF STANDARDS-1963-A

AD A118041



①

DTC FILE COPY

UNITED STATES AIR FORCE
AIR UNIVERSITY
AIR FORCE INSTITUTE OF TECHNOLOGY
Wright-Patterson Air Force Base, Ohio

This document has been approved
for public release and sale; its
distribution is unlimited.

DTIC
ELECTE
AUG 11 1982

E

82 08 11 046

AFIT/GEP/PH/81D-2

①

MODE ANALYSIS IN A
MISALIGNED UNSTABLE RESONATOR

THESIS

AFIT/GEP/PH/81D-2

Richard W. Berdine
1Lt USAF

This document has been approved
for public release and sale; its
distribution is unlimited.

DTIC
ELECTE
AUG 11 1982
S D E

MODE ANALYSIS IN A
MISALIGNED UNSTABLE RESONATOR

THESIS

Presented to the Faculty of the School of Engineering
of the Air Force Institute of Technology
Air University
in Partial Fulfillment of the
Requirements for the Degree of
Master of Science

by

Richard W. Berdine, B.S.
1Lt USAF
Graduate Engineering Physics
December 1981

Accession For	
NTIS GRA&I	<input checked="checked" type="checkbox"/>
DTIC TAB	<input type="checkbox"/>
Unannounced	<input type="checkbox"/>
Justification	
By _____	
Distribution/	
Availability Codes	
Dist	Avail and/or Special
A	



Approved for public release; distribution unlimited

PREFACE

The purpose of this study was to analyze the effects of mirror misalignment on the transverse modes and beam steering of an unstable laser resonator. The analysis was developed for any general unstable resonator design with rectangular apertures and did not allow for inclusion of a gain medium. The final result, a computer program, can be used to calculate mode eigenvalues and subsequently the intensity and phase in the plane of the feedback mirror for a desired mode. The slope of the phase, from which a beam steering angle can be determined, is also calculated for the lowest loss mode. The resulting tilt in the phase front is due to diffraction, and is consequently a beam steering angle additional to the geometric misalignment. The code is basically an extension, or modification, to a previous computer model developed by J.E. Rowley, and follows similar work done by P. Horwitz.

Although a major portion of this work may be found elsewhere, specific details and applications throughout the text are generally not available. They are provided here in order to present a complete and clear progression of the analysis. A large number of equations and derivations are required since the topic is analytical in nature rather than experimental. This sometimes leads to trivial substitutions and algebraic steps being included for the sake of continuity, but it is hoped that these are minimal. Physical interpretations and definitions are included where possible for better understanding.

I would like to express my gratitude to my advisor, Lt. Col. John Erkkila, for his time, patience, guidance, and especially his enthusiasm which inspired me continually throughout.

Table of Contents

Preface	ii
List of Figures	v
Abstract	vii
I. Introduction	1
Background	1
Objectives	6
Assumptions	7
Procedure and Organization	8
II. Development of the Integral Equation from the Fresnel - Kirchhoff Diffraction Formula	9
1-D Analysis	9
Introduction of Phase Lag	12
III. The Integral Equation Appropriate to the Misaligned Resonator	19
Effects of Mirror Misalignment	19
IV. Solution of the Generalized Integral Equation	24
Stationary Phase Approximation	24
The Polynomial Equation	28
Second Order Approximation	30
V. Beam Steering	33
Geometrical Beam Steering	33
Beam Steering Angles Due to Diffraction	35
VI. Results, Conclusions, and Recommendations	38
Results	38
Conclusions	39
Recommendations	40
Bibliography	46
Appendix A (Solution of definite integral in equation (2.23)) .	48
Appendix B (Final form of the integral equation)	51
Appendix C (The polynomial equation)	53

Appendix D (The plots of higher order modes)	55
Appendix E (Program listing)	61
Vita	75

List of Figures

<u>Figure</u>	<u>Page</u>
1-1 Stable and unstable resonator geometries	2
1-2 Equivalent lens system of an unstable resonator . . .	3
2-1 Geometry of rectangular plane mirrors	10
2-2 Typical unstable resonator geometry (for phase lag) . .	11
3-1 Geometry of an unstable laser resonator (misaligned) . .	20
5-1 Equivalent asymmetric cavity of the misaligned resonator	35
6-1 Intensity plot for the lowest loss mode with $\delta = 0.0$.	41
6-2 Phase plot for the lowest loss mode with $\delta = 0.0$. . .	41
6-3 Intensity plot for the lowest loss mode with $\delta = 0.2$.	42
6-4 Phase plot for the lowest loss mode with $\delta = 0.2$. . .	42
6-5 Intensity plot for the lowest loss mode with $\delta = 0.5$.	43
6-6 Phase plot for the lowest loss mode with $\delta = 0.5$. . .	43
6-7 Phase slope vs. mirror misalignment (magnification = 2.0 and Equivalent Fresnel number = 9.6)	44
6-8 Phase slope vs. mirror misalignment (magnification = 2.9 and Equivalent Fresnel number = 16.4)	45
D-1 Intensity plot for mode #2 and $\delta = 0.0$	56
D-2 Phase plot for mode #2 and $\delta = 0.0$	56
D-3 Intensity plot for mode #2 and $\delta = 0.5$	57
D-4 Phase plot for mode #2 and $\delta = 0.5$	57
D-5 Intensity plot for mode #3 and $\delta = 0.0$	58
D-6 Phase plot for mode #3 and $\delta = 0.0$	58
D-7 Intensity plot for mode #3 and $\delta = 0.5$	59
D-8 Phase plot for mode #3 and $\delta = 0.5$	59

<u>Figure</u>		<u>Page</u>
D-9	Intensity plot across the feedback mirror only using the first order approximation	60
D-10	Phase plot across the feedback mirror only using the first order approximation	60

ABSTRACT

The integral equation that describes mode structure of an unstable resonator with rectangular apertures is developed from scalar diffraction theory. This equation, modified to account for misalignments, is solved by applying the asymptotic methods developed by Horwitz. A second order approximation of the method of stationary phase is then employed to calculate phase and intensity values for all points in the output plane. The phase front is also curve fitted to a straight line over the geometrical region for the lowest loss mode. From the slope of the straight line, a direction of propagation can be attributed to the wave. This is a diffracted beam steering angle and is additional to the geometric steering angle (i.e., the beam steering angle due to the geometric misalignment of either or both mirrors).

Plots of intensity and phase for various degrees of misalignments are presented as results of a computer program that utilizes the derived expressions. Also included are graphs of the phase slope versus mirror misalignment.

MODE ANALYSIS IN A MISALIGNED UNSTABLE RESONATOR

I. Introduction

Background

In any laser cavity there are two modes of oscillation: longitudinal (or axial) and transverse (or radial). The longitudinal modes coupled with a specific transverse mode determine the frequency of radiation emitted, while the transverse modes alone determine the intensity distribution across the laser beam. In either case, the existing modes can be found by applying the appropriate boundary conditions to the wave equation. In a stable resonator with spherical mirrors and edge effects (diffraction effects due to the finite size of the mirrors) neglected, the transverse solutions to the wave equation become Hermite-Gaussian or Laguerre-Gaussian functions for mirrors with either rectangular or circular symmetry respectively (Ref. 1:1324).

For the unstable resonator, edge effects must be included since the output is a diffraction-coupled beam passing around, rather than through the output mirror. An iterative approach to finding the resonant modes of the cavity accounts for these edge effects and was introduced by Fox and Li (Ref. 2). This method is to first assume an initial field distribution in the resonator and then apply the Fresnel-Kirchhoff diffraction formula to the problem of infinite strip mirrors.

Figure 1-1 shows differences between a stable resonator and an unstable resonator. Any ray originating in the stable resonator and striking one of the mirrors will remain inside the cavity, even for an infi-

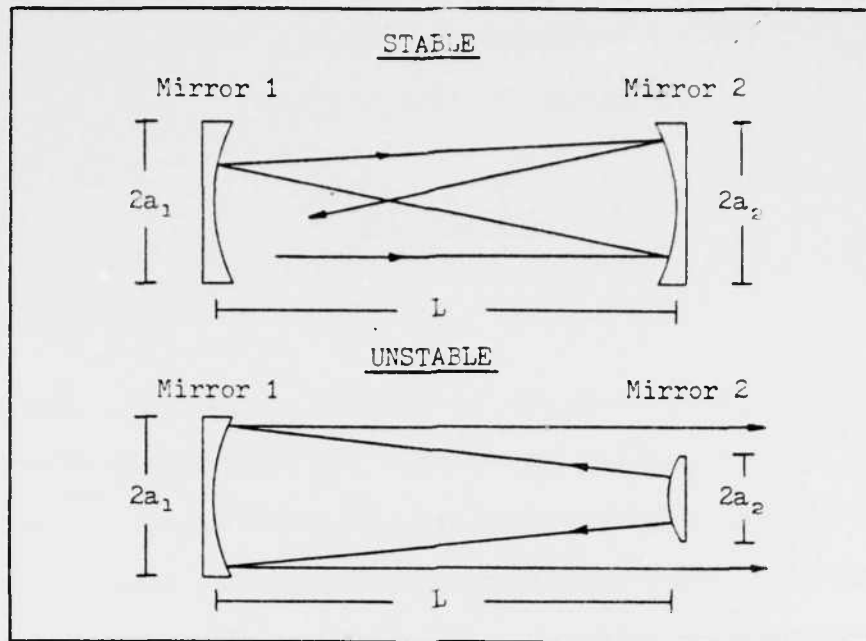


Fig. 1-1. Typical stable and unstable resonator geometries.

nite number of passes. In the unstable resonator however, the ray will eventually pass out of the cavity. For the case under consideration, a_1 assumed large in comparison with beam spot size on mirror 1, the ray will pass around the much smaller feedback mirror. It can therefore be seen that only edge effects from the smaller mirror need to be considered.

The more familiar criterion for stable and unstable resonators is given by the product of g_1 and g_2 , where

$$g_i = 1 - \frac{L}{R_i} \quad i = 1, 2 \quad (1.1)$$

Here L = cavity length and R_i = radius of curvature of the i^{th} mirror. Also, R_i is defined as positive for concave mirrors and negative for convex. For stable resonators the product of the g parameters lies inside the range of

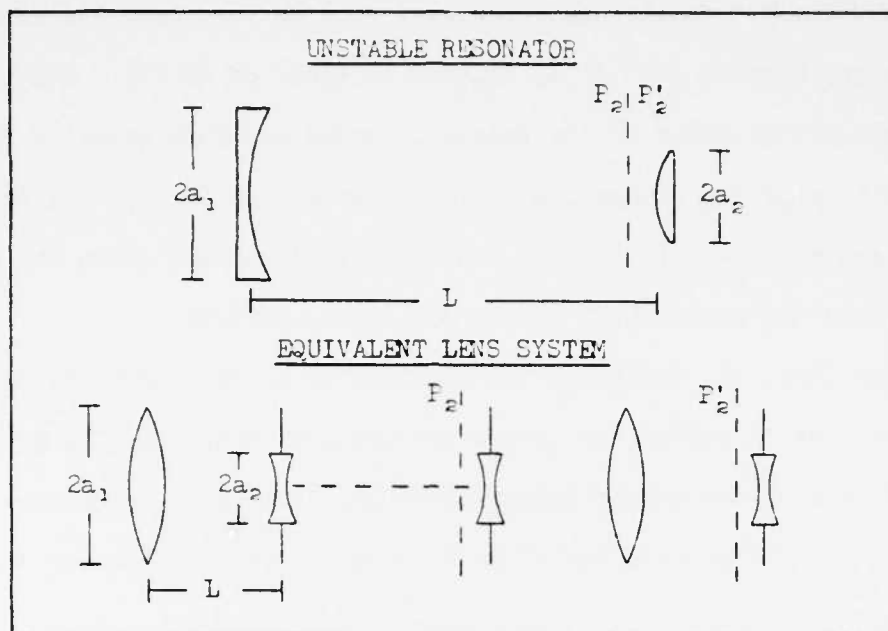


Fig. 1-2. Equivalent lens system of an unstable resonator.

$$0 \leq g_1 g_2 \leq 1 \quad (1.2)$$

Unstable resonators however, are characterized by either $g_1 g_2 > 1$ or $g_1 g_2 < 0$.

The equivalent lens train of a typical unstable resonator is shown in Figure 1-2. As stated earlier, an initial field distribution is assumed at P_2 and propagated through one round trip to P'_2 using the Fresnel-Kirchhoff diffraction formula. With the restriction that the field reproduce itself after the round trip and introducing phase lag due to mirror curvature, the resulting integral equation is

$$v g(x) = \sqrt{\frac{it}{\pi}} \int_{-1}^1 g(y) e^{-it(y - x/M)^2} dy \quad (1.3)$$

Here x is the spatial coordinate, y is a dummy variable of integra-

tion, $i = \sqrt{-1}$, M = cavity magnification, $g(x)$ is the field distribution on the output mirror, and t is defined in equation (B.10). The transverse field distribution of the resonator modes are then given by the eigenfunctions of the integral equation. The multiplicative constant, v , is the eigenvalue associated with the eigenfunctions and gives the diffraction loss and phase shift of the mode (Ref. 1:1325).

Rowley (Ref. 3), following the analysis of Horwitz (Ref.4), developed a computer code to numerically solve the integral equation. He assumed that the field on the mirror before the round trip, $g(y)$, consisted of a unit amplitude cylindrical wave plus a series of edge diffracted waves, and is given by

$$g(y) = 1 + \sum_{n=1}^N c_n H_n(y) \quad (1.4)$$

(Ref. 3:17). Therefore, the field on the mirror after the round trip, $g(x)$, would differ only by the multiplicative constant v .

Letting

$$c_n H_n(y) = a_n F_n(y) + b_n G_n(y) \quad (1.5)$$

the integral equation to be solved is

$$v \left\{ 1 + \sum_{n=1}^N [a_n F_n(x) + b_n G_n(x)] \right\} = \sqrt{\frac{it}{\pi}} \int_{-1}^1 e^{-it(y - x/M)^2} \left\{ 1 + \sum_{n=1}^N [a_n F_n(y) + b_n G_n(y)] \right\} dy \quad (1.6)$$

The method of stationary phase is used to approximate this integral.

It states that an integral of the form

$$I = \int_a^b e^{-itp(y)} q(y) dy \quad (1.7)$$

can be expressed as a series when t is large and $q(y)$ is a slowly varying function. The first two terms of the series are given by

$$I \approx e^{-i\pi/4} q(y_0) e^{-itp(y_0)} \sqrt{\frac{2\pi}{tp''(y_0)}} + \frac{i}{t} \left[\frac{q(b)}{p'(b)} e^{-itp(b)} - \frac{q(a)}{p'(a)} e^{-itp(a)} \right] \quad (1.8)$$

(Ref. 3:19; 14:1073). This is a first order approximation to the integral equation and is used in Chapter 4 for determination of eigenvalues. A second order approximation is also given in Chapter 4 and is required for intensity and phase calculations outside the mirror edges. In equation (1.8) the prime indicates the derivative of the function with respect to y , and y_0 is the stationary phase point, i.e.,

$$p'(y_0) = 0 \quad (1.9)$$

Before equation (1.6) can be solved, explicit forms for $F_n(y)$ and $G_n(y)$ are needed. They are

$$F_n(y) = -\sqrt{\frac{M_{n-1}}{4i\pi t}} \frac{\exp[-it(1 - y/M^n)^2/M_{n-1}]}{1 - y/M^n} \quad (1.10)$$

and

$$G_n(y) = - \sqrt{\frac{M_{n-1}}{4i\pi t}} \frac{\exp[-it(1 + y/M^n)/M_{n-1}]}{1 + y/M^n} \quad (1.11)$$

(Ref. 3:20; 4:1531), where the variable M_n is defined in equation (3.12). Horwitz determined the functional form of the F_n 's and G_n 's by an asymptotic expansion of the integral equation (Ref. 4). The specific set of functions were then chosen for their reproducibility, i.e., after making the stationary phase approximation to equation (1.6) the same set of functions are arrived at. Equating coefficients then leads to a $2N + 1$ degree polynomial in v , which is solved by a generalized root finding routine. Once the eigenvalues have been determined, the field is calculated by first specifying a particular eigenvalue or mode and then calculating the constants a_n and b_n (a detailed solution is left to Chapter 4).

A limitation to this analysis is the fact that it is only valid for cavities with perfectly aligned mirrors. Since mirror alignment is critical to the effectiveness of any laser system, it is desirable to be able to determine the sensitivity of the system for a specified misalignment. This sensitivity is measured in terms of the power out, beam steering, and mode distortion (i.e., the beam quality). Several investigations into mode distortion due to mirror misalignment have been reported (Ref. 5, 6,7,8), however, only a few have dealt with the problem of beam steering (Ref. 8).

Objectives

The purpose of this study is to analyze the effects of mirror misalignment on the transverse modes and beam steering of an unstable laser resonator. The analysis is developed for a bare strip resonator with

rectangular apertures following similar work done by Horwitz (Ref. 5).

A computer program was written (a modified version of a code developed by Rowley) to facilitate the study. The computer model calculates mode eigenvalues and subsequently evaluates the intensity and phase in the plane of the feedback mirror for a desired mode. The slope of the phase, from which the direction of propagation can be determined, is also calculated for the lowest loss mode. The resulting tilt in the phase front is due to diffraction, and is a beam steering angle additional to the geometric misalignment.

Assumptions

The basic assumptions of Reference 3 are still invoked since the analysis is an extension of this previous work. In addition to these is the added restriction of small misalignments (Assumption 5). They are (Ref. 3:2) :

1. That scalar diffraction theory can be used if a) the diffracting aperture is large compared to wavelength and b) the diffracted fields are not observed too close to the aperture. The first constraint is easily attained at optical wavelengths and the second is achieved at moderate cavity lengths.
2. That the diffraction integrals and mode eigenfunctions are separable allowing a 1-D strip resonator to be used in the foregoing analysis. When the mirror separation is very much larger than the mirror dimensions, the problem of the rectangular mirrors reduces to a one-dimensional problem of infinite strip mirrors (Ref. 2:457).
3. Diffraction effects from only the feedback mirror are considered if the larger mirror is considered infinite in comparison with the beam

spot size on that mirror.

4. That the modes in the strip resonator consist of a fundamental cylindrical wave modified by a finite number of edge diffraction effects. This assumption is supported by early analysis of unstable resonators (Ref. 9:279).

5. That the optical axis (the line joining the centers of curvature of the two mirrors) does not pass too close (within a Fresnel zone) to the edge of the small mirror (Ref. 5:167).

Procedure and Organization

In Chapter 2 the Fresnel-Kirchhoff diffraction formula is modified to include phase lag due to mirror curvature for a strip resonator; and in Chapter 3 the resulting integral equation is generalized to include effects of small misalignments. Chapter 4 then deals with its solution using the stationary phase approximation. In Chapter 5 the diffracted beam steering angle is presented and the magnitude compared to the geometric beam steering angle, while the results and conclusions are left to Chapter 6.

II. Development of the Integral Equation
from the
Fresnel-Kirchhoff Diffraction Formula

Equation (1.3) is derived by first reducing the problem of rectangular mirrors to a one-dimensional problem of infinite strip mirrors. This analysis follows the work of Fox and Li (Ref. 2). The next step is to account for phase lag due to mirror curvature, which can be found in References 3 and 4. Although this derivation can be found in the references cited, it is included here for easy access and completeness of the study.

1-D Analysis (Ref. 2:456-457, 484-486)

In a Cartesian coordinate system, the field E_p due to an illuminated aperture A is given by the surface integral

$$E_p(x,y) = \frac{ik}{4\pi} \int_A E_a(x,y) \frac{e^{-ikr}}{r} (1 + \cos\theta) dS \quad (2.1)$$

where E_a is the aperture field, k is the propagation constant, r is the distance from a point on the aperture to the point of observation, and θ is the angle which r makes with the unit normal to the aperture. From Figure 2-1, where propagation is from right to left, this can be written as

$$E(x_1, y_1) = \frac{i}{2\lambda} \int_{-c}^c \int_{-a}^a E(x_2, y_2) \frac{e^{-ikr}}{r} \left(1 + \frac{L}{r}\right) dx_2 dy_2 \quad (2.2)$$

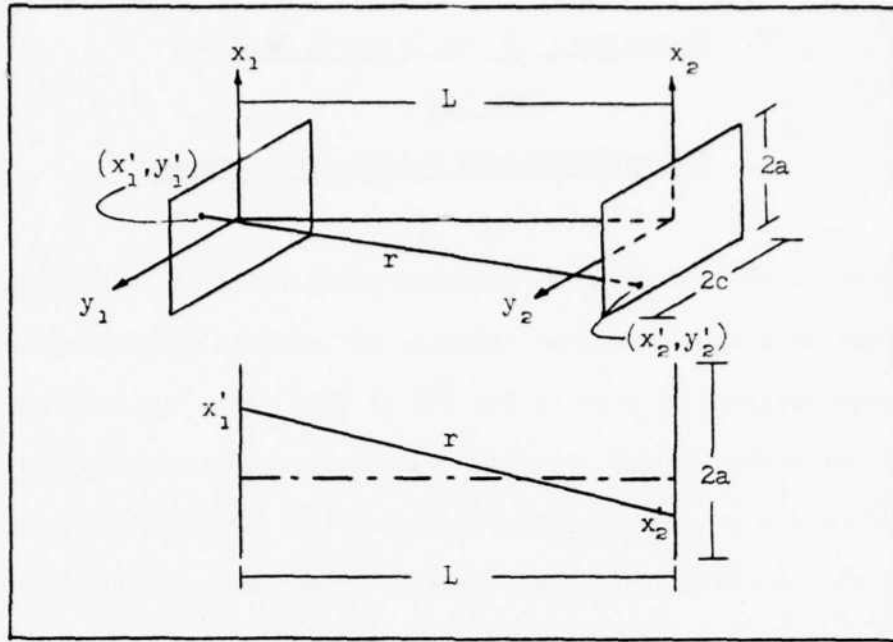


Fig. 2-1. Geometry of rectangular plane mirrors.

Also λ is the wavelength of the radiation and r is the distance defined by

$$r = \sqrt{L^2 + (x_2 - x_1)^2 + (y_2 - y_1)^2} \quad (2.3)$$

If L is large compared to the dimensions of the diffracting aperture, mirror 2, then the binomial expansion of the above square root can be approximated by retaining only the first two terms of the expansion, i.e.

$$r \approx L \left[1 + \frac{1}{2} \left(\frac{x_2 - x_1}{L} \right)^2 + \frac{1}{2} \left(\frac{y_2 - y_1}{L} \right)^2 \right] \quad (2.4)$$

where L^2 was factored out of the square root before the expansion. If again L is considered large compared to dimensions a and c , then $\cos \theta \approx \frac{r}{L} \approx 1$. It is seen here that even though $r \approx L$, the exponential

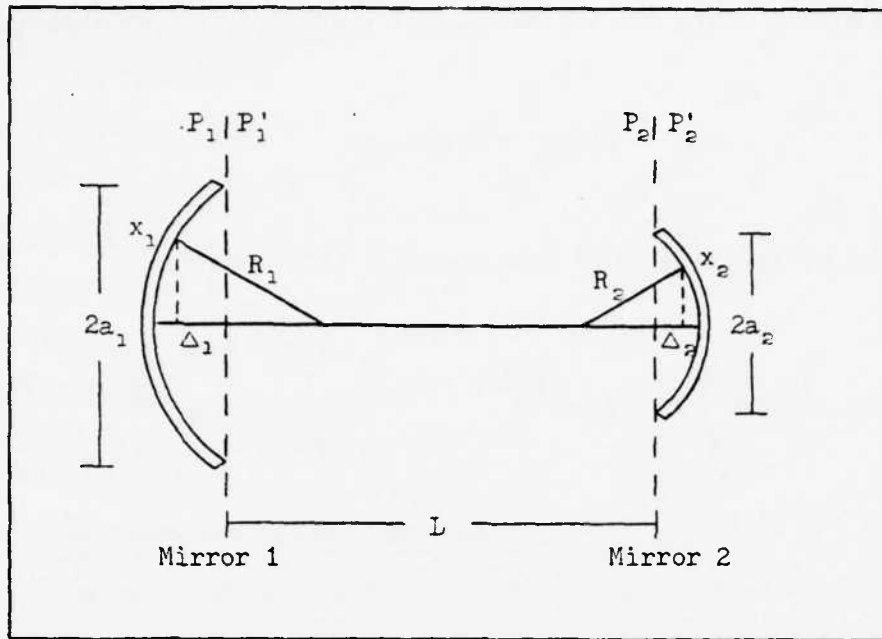


Fig. 2-2. Typical unstable resonator geometry.

will be more sensitive to this round-off, therefore equation (2.4) is substituted into equation (2.2) to become

$$E(x_1, y_1) = \frac{ie^{-ikL}}{\lambda L} \int_{-c}^c \int_{-a}^a E(x_2, y_2) e^{-\frac{ik}{2L}[(x_2 - x_1)^2 + (y_2 - y_1)^2]} dx_2 dy_2 \quad (2.5)$$

The resonant modes of any laser cavity are characterized by reproducible fields after only one round trip through the resonator. From Figure 2-2 this is given by

$$\gamma E(x'_2, y'_2) = E(x_2, y_2) \quad (2.6)$$

Here $E(x'_2, y'_2)$ is the field after the round trip at P'_2 , $E(x_2, y_2)$ is the original field at P_2 , and γ is a complex constant. When the mirrors have rectangular geometry the fields are best represented in a Cartesian

coordinate system where the two orthogonal components become separable.

$$E(x,y) = U(x) U(y) \quad (2.7)$$

Substitution of equation (2.7) into equation (2.5) yields

$$U(x_1)U(y_1) = \frac{ie^{-ikL}}{\lambda L} \int_{-a}^a U(x_2) e^{-\frac{ik}{2L}(x_2 - x_1)^2} dx_2 \int_{-c}^c U(y_2) e^{-\frac{ik}{2L}(y_2 - y_1)^2} dy_2 \quad (2.8)$$

Restricting the analysis to a one-dimensional strip resonator with the integral defined over the region of the diffracting aperture, mirror 2, the equation for the one-way diffraction of a wave from P_2 to P_1 becomes

$$U(x_1) = \sqrt{\frac{i}{\lambda L}} e^{-\frac{ikL}{2}} \int_{-a_2}^{a_2} U(x_2) e^{-\frac{ik}{2L}(x_2 - x_1)^2} dx_2 \quad (2.9)$$

Similarly, the one-way diffraction formula for propagation from P'_1 to P'_2 is

$$U(x'_2) = \sqrt{\frac{i}{\lambda L}} e^{-\frac{ikL}{2}} \int_{-a_1}^{a_1} U(x'_1) e^{-\frac{ik}{2L}(x'_1 - x'_2)^2} dx'_1 \quad (2.10)$$

Introduction of Phase Lag

For equations (2.9) and (2.10) to adequately represent propagation in the resonator, the phase lag due to mirror curvature must be accounted for. Considering equation (2.9), or propagation from mirror 2 to mirror 1 in Figure 2-2, the total phase lag at some position x is

$$\phi(x) = k[\Delta_1 - \Delta(x_1) + \Delta_2 - \Delta(x_2)] \quad (2.11)$$

or

$$\phi(x) = k[R_1 - \sqrt{R_1^2 - x_1^2} + R_2 - \sqrt{R_2^2 - x_2^2}] \quad (2.12)$$

The maximum free space region between plane P_i and the i^{th} mirror is Δ_i , while $\Delta(x_i)$ is the free space region between plane P_i and the i^{th} mirror at some distance x_i . It should be emphasized that this is the phase lag for propagation in one direction only.

We can assume the paraxial approximation to be valid over the entire mirror if the radius of curvature is large and the physical dimensions are small compared to the resonator length. Therefore, if the above square roots are expanded in a binomial series as before, only the first two terms are retained.

$$\sqrt{1 - x_1^2/R_1^2} \approx 1 - x_1^2/2R_1^2 \quad (2.13)$$

Equation (2.12) is now written

$$\phi(x) = k(x_1^2/2R_1 + x_2^2/2R_2) \quad (2.14)$$

Writing $1/R_i$ in terms of the g parameter from equation (1.1), the phase lag takes the form

$$\phi(x) = \frac{k}{2L}[x_1^2(1 - g_1) + x_2^2(1 - g_2)] \quad (2.15)$$

This phase term, seen to be positive, is actually a phase advance-

ment; but when added to the negative phase of equation (2.9) it gains the awkward notation of phase lag. The total phase for the one-way diffraction of a wave as it applies to a resonator with spherical mirrors is then

$$\phi_{\text{total}} = -\frac{k}{2L}[x_1^2 + x_2^2 - 2x_1x_2 - x_1^2(1 - \epsilon_1) - x_2^2(1 - \epsilon_2)] \quad (2.16)$$

After combining some terms, the diffraction formula for propagation from P_2 to P_1 is given by

$$U(x_1) = \sqrt{\frac{i}{\lambda L}} e^{-\frac{ikL}{2}} \int_{-a_2}^{a_2} U(x_2) e^{-\frac{ik}{2L}(x_1^2 \epsilon_1 + x_2^2 \epsilon_2 - 2x_1x_2)} dx_2 \quad (2.17)$$

Similarly equation (2.10) becomes

$$U(x'_2) = \sqrt{\frac{i}{\lambda L}} e^{-\frac{ikL}{2}} \int_{-a_1}^{a_1} U(x'_1) e^{-\frac{ik}{2L}(x_1'^2 \epsilon_1 + x_2'^2 \epsilon_2 - 2x_1'x_2')} dx'_1 \quad (2.18)$$

If the reproducibility argument of equation (2.6) is invoked, i.e.,

$$\gamma' U(x'_1) = U(x_1) \quad (2.19)$$

then equations (2.17 - 2.19) can be combined to yield the round trip diffraction formula as it applies to a laser resonator with spherical mirrors and rectangular apertures. In the equation below, the constant phase term has been absorbed into the complex constant γ' to become γ . The integral equation is

$$\begin{aligned}
 \gamma U(x'_2) = \frac{i}{\lambda L} \int_{-a_1}^{a_1} \int_{-a_2}^{a_2} U(x_2) e^{-\frac{ik}{2L}(x_1'^2 \xi_1 + x_2'^2 \xi_2 - 2x_1' x_2')} \\
 e^{-\frac{ik}{2L}(x_1^2 \xi_1 + x_2^2 \xi_2 - 2x_1 x_2)} dx_1' dx_2 \quad (2.20)
 \end{aligned}$$

This equation, although derived from the geometry of Figure 2-2, is equally valid for the resonator of Figure 1-2 and, in general, any laser resonator. This can be seen from the sign convention chosen for the radius of curvature, R_1 . In the above example R_1 and R_2 are defined as positive (refer to page 2) leading to a direct substitution, from equation (2.14) to equation (2.15), of $1/R_1$ in terms of ξ_1 . From Figure 1-2 however, equation (2.14) takes the form

$$\phi(x) = k(x_1^2/2R_1 - x_2^2/2R_2) \quad (2.21)$$

But with $1/R_2 = (\xi_2 - 1)/L$, the phase again takes the form of equation (2.15). Thus equation (2.20) is a general result where the sign of R_1 has been absorbed into the ξ parameter.

The next step is to consider diffraction effects from the feedback mirror only. This permits the limits of integration over P_1 to go to infinity since the beam spot size on mirror 1 is assumed small compared to mirror dimensions. If in addition to setting the limits of integration over mirror 1 to $\pm \infty$, we let

$$\begin{aligned}
 x_1' &= x_1 \\
 x_2' &= x \\
 x_2 &= y
 \end{aligned} \quad (2.22)$$

the integral equation becomes

$$\gamma U(x) = \frac{i}{\lambda L} \int_{-a_2}^{a_2} \int_{-\infty}^{\infty} U(y) e^{-\frac{ik}{2L}(x_1^2 \xi_1 + x^2 \xi_2 - 2x_1 x)} e^{-\frac{ik}{2L}(x_1^2 \xi_1 + y^2 \xi_2 - 2x_1 y)} dx_1 dy \quad (2.23)$$

The justification for equations (2.22) is seen by following a single ray from mirror 2 to mirror 1 and then back again. As the ray strikes mirror 1 the point of incidence must be the same as the point of reflection, i.e., $x_1 = x'_1$. However, the ray leaving mirror 2 will in general be displaced from the original position giving $x_2 \neq x'_2$. Therefore, if x'_2 is the x position at which the field is to be calculated after the round trip and $x_2 = y$ (where y is a dummy variable of integration over the diffracting aperture), equation (2.20) becomes equation (2.23) above.

The interior integral is extracted with its evaluation relegated to Appendix A; the result being the complete kernel of the integral equation.

$$K = \sqrt{\frac{i}{2\lambda L \xi_1}} e^{-\frac{i\pi}{2\lambda L \xi_1} [(2\xi_1 \xi_2 - 1)(x^2 + y^2) - 2xy]} \quad (2.24)$$

Now if

$$g = 2\xi_1 \xi_2 - 1 \quad (2.25a)$$

and

$$F = \frac{F_2}{2\xi_1} = \frac{a_2^2}{2\lambda L \xi_1} \quad (2.25b)$$

are introduced, the round trip diffraction formula becomes

$$\gamma U(x) = \sqrt{\frac{iF}{a_2}} \int_{-a_2}^{a_2} U(y) e^{-\frac{i\gamma F}{a_2^2} [g(x^2 + y^2) - 2xy]} dy \quad (2.26)$$

All quantities are the same as defined previously with the addition of F_2 . Here F_2 is the ordinary Fresnel number of the smaller mirror. The ordinary Fresnel number is physically interpreted as the additional path length per pass in half wavelengths for a ray traveling from one mirror's center to the other mirror's edge, compared to one traveling from mirror center to mirror center (Ref. 11:159-161).

Normalizing the coordinate system such that $a_2 = 1$, the resulting integral equation is

$$\gamma U(x) = \sqrt{iF} \int_{-1}^1 U(y) e^{-i\pi F [g(x^2 + y^2) - 2xy]} dy \quad (2.27)$$

Further simplification is obtained by defining

$$N_{eq} = \frac{F}{2}(M - 1/M) \quad (2.28)$$

and

$$U(x) = e^{-i\pi N_{eq} x^2} g(x) \quad (2.29)$$

Several different interpretations for the equivalent Fresnel number, N_{eq} , are available (Ref. 11:159-161; 12:360). Here the equivalent Fresnel number is defined as the distance, in half wavelengths, between the outer edge of the output mirror and the nearest point on the outgoing geometrical wave when that wave just touches the mirror center (Ref. 12:360). That geometrical wave is assumed to be a cylindrical wave of the

form

$$e^{-i\pi N_{eq} x^2} \quad (2.30)$$

Substitution of equations (2.28) and (2.29) into equation (2.27) yields

$$\gamma g(x) e^{-\frac{i\pi F}{2}(M - \frac{1}{M})x^2} = \sqrt{iF} \int_{-1}^1 g(y) e^{-\frac{i\pi F}{2}(M - \frac{1}{M})y^2} e^{-i\pi F[g(x^2 + y^2) - 2xy]} dy \quad (2.31)$$

After some manipulation, detailed in Appendix B, this equation simplifies to the final form

$$v g(x) = \sqrt{\frac{it}{\pi}} \int_{-1}^1 g(y) e^{-it(y - x/M)^2} dy \quad (2.32)$$

where from Appendix B, $t = \pi M F$ and $v = \gamma \sqrt{M}$.

III. The Integral Equation Appropriate to the Misaligned Resonator

In Chapter 2 the integral equation was developed for the case of a perfectly aligned resonator. It has been shown (Ref. 5:167-168; 10:2241-2242) that the equation appropriate to the general misaligned resonator differs from the usual one only in the limits of integration. This is true regardless of which mirror is tilted.

The limits of integration are determined by the angle through which the mirror is tilted, which mirror is misaligned, and the cavity geometry. The results of this section (i.e., the limits of integration) pertain only to the geometry of Figure 3-1 and cannot be generalized to include other configurations.

Effects of Mirror Misalignment

This analysis is basically a geometry problem with the development restricted to misalignment of the feedback mirror.

In Figure 3-1 the optic axis of the perfectly aligned resonator is the line \overline{bcde} . When mirror 2 is tilted around point c by an angle θ , the optic axis of the resonator becomes \overline{hgfe} . The center of curvature of mirror 1 is at e, while the centers of curvature of mirror 2 before and after the tilt are d and f, respectively. The angle between the new optic axis and the old is ω . For small angles θ , ω is given by

$$\omega = \overline{df}/\overline{ed} = \frac{\theta R_2}{R_1 - R_2 - L} \quad (3.1)$$

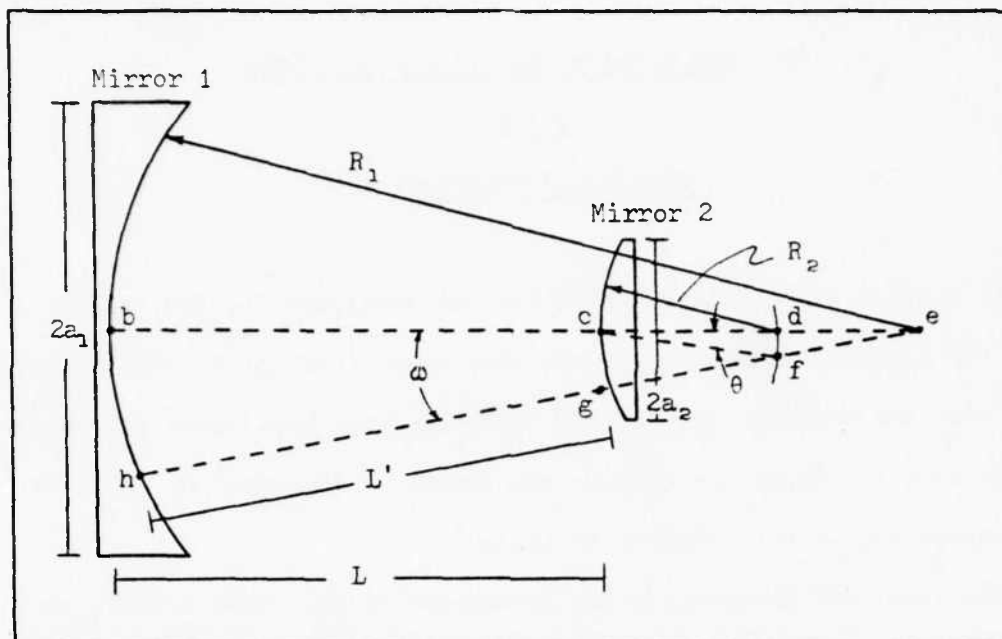


Fig. 3-1. Geometry of an unstable laser resonator.

This, however, neglects the fact that R_2 by convention is negative. Therefore, substitution of a negative R_2 and rewriting in terms of the g parameter, equation (3.1) becomes

$$\omega = \theta \frac{g_1 - 1}{1 - g_1 g_2} \quad (3.2)$$

The degree of tilt, as expressed in distance across the feedback mirror, is given by the line $\overline{cē}$. This distance is

$$\overline{cē} = \omega(R_1 - L') \approx \omega(R_1 - L) \quad (3.3)$$

If we again write R_1 in terms of g_1 and use the results of equation (3.2), it becomes

$$\overline{c\bar{g}} = \frac{\theta L \xi_1}{\xi_1 \xi_2 - 1} \quad (3.4)$$

The problem now is to express the distance $\overline{c\bar{g}}$ in terms of the mirror dimension a_2 .

$$\frac{\overline{c\bar{g}}}{a_2} = \frac{L\theta}{a_2} \frac{\xi_1}{\xi_1 \xi_2 - 1} \quad (3.5)$$

From equation (2.25) this is written

$$\frac{\overline{c\bar{g}}}{a_2} = \frac{\theta}{2F} \frac{a_2/\lambda}{\xi_1 \xi_2 - 1} \quad (3.6)$$

With the following definitions

$$N_{eq} = \frac{1}{2} F(M - 1/M) \quad (3.7a)$$

and

$$M = \frac{(\xi_1 \xi_2)^{\frac{1}{2}} + (\xi_1 \xi_2 - 1)^{\frac{1}{2}}}{(\xi_1 \xi_2)^{\frac{1}{2}} - (\xi_1 \xi_2 - 1)^{\frac{1}{2}}} \quad (3.7b)$$

equation (3.6) takes the form

$$\delta = \frac{\overline{c\bar{g}}}{a_2} = \frac{a_2}{\lambda} \frac{\theta}{N_{eq}} \frac{M+1}{M-1} \quad (3.8)$$

When the angle θ is small, the tilted resonator is equivalent to an aligned resonator with an asymmetric mirror relative to the resonator axis (Ref. 10:2242), refer to Figure 5-1. Since the origin of the x-axis is defined as the point of intersection of the optic axis and mir-

ror 2, the extent of the asymmetric mirror is from $-1 + \delta$ to $1 + \delta$.

The limits of integration are now

$$\alpha = -1 + \delta \quad (3.9a)$$

and

$$\beta = 1 + \delta \quad (3.9b)$$

Although δ is in general a linear function of θ for any cavity configuration, its exact form must be determined from the specific geometry.

The generalized integral equation is now written as

$$v_g(x) = \sqrt{\frac{it}{\pi}} \int_{\alpha}^{\beta} g(y) e^{-it(y - x/M)^2} dy \quad (3.10)$$

The series functions F_n and G_n also have minor changes due to the misalignment, i.e.,

$$F_n(x) = - \sqrt{\frac{M_{n-1}}{4it}} \frac{\exp[-it(\beta - x/M^n)^2/M_{n-1}]}{\beta - x/M^n} \quad (3.11a)$$

and

$$G_n(x) = \sqrt{\frac{M_{n-1}}{4it}} \frac{\exp[-it(\alpha - x/M^n)^2/M_{n-1}]}{\alpha - x/M^n} \quad (3.11b)$$

(Ref. 5:168-169), where again M is the cavity magnification and

$$M_n = \sum_{k=0}^n M^{-2k} \quad (3.12)$$

As previously stated, δ is a function of which mirror is tilted.

If mirror 1 had been misaligned by the same angle θ , then it would have been found (Ref. 8:579) that

$$\overline{cg} = \frac{\theta R_1 R_2}{L - R_1 - R_2} = \frac{\theta L}{\xi_1 \xi_2 - 1} \quad (3.13)$$

It is evident from equations (3.4) and (3.13), that the geometry of Figure 3-1 is less sensitive to misalignment (by a factor of ξ_1) for a tilt of mirror 2 vs. the same tilt of mirror 1 .

IV. Solution of the Generalized Integral Equation

In Chapter 3 the integral equation was modified to include effects of small misalignments. This chapter is concerned with its solution by applying the method of stationary phase.

Since the problem is basically algebraic and requires numerous manipulations, the scope of this section is limited to a detailed outline of the solution.

Stationary Phase Approximation

The integral equation to be solved is

$$v g(x) = \sqrt{\frac{it}{\pi}} \int_{\alpha}^{\beta} g(y) e^{-it(y - x/M)^2} dy \quad (4.1)$$

where $g(x)$ is the field distribution on the output mirror after the round trip, $g(y)$ is the original field distribution, and v is the eigenvalue associated with the eigenfunctions.

Following Chapter 1,

$$g(y) = 1 + \sum_{n=1}^N c_n H_n(y) \quad (4.2)$$

where it was assumed that $g(y)$ consisted of a unit amplitude cylindrical wave plus a series of edge diffracted waves. The basis for this assumption is that the original field is composed of the primary cylindrical wave plus diffraction effects from the previous N reflections. The series terminates with $H_N(y)$, the last function to have an effect on the

field. The addition of one more function (or reflection) to the series would add only to the amplitude and not the spatial distribution or shape of the field, i.e., $H_{N+1}(y)$ is a constant. A good approximation is to let

$$N \geq \frac{\ln(250 N_{eq})}{\ln M} \quad (4.3)$$

(Ref. 4:1533).

Combining equations (1.5), (4.1), and (4.2) yields

$$v \left\{ 1 + \sum_{n=1}^N [a_n F_n(x) + b_n G_n(x)] \right\} = \sqrt{\frac{it}{\pi}} \int_{\alpha}^{\beta} e^{-it(y - x/M)^2} \left\{ 1 + \sum_{n=1}^N [a_n F_n(y) + b_n G_n(y)] \right\} dy \quad (4.4)$$

This is equivalent to equation (1.6) with the limits of integration changed to account for the misalignment. Substitution of the F_n 's and G_n 's from equation (3.11) allows the stationary phase approximation to be applied, refer to equation (1.8). Defining the quantities

$$I_0 = \sqrt{\frac{it}{\pi}} \int_{\alpha}^{\beta} e^{-it(y - x/M)^2} dy \quad (4.5a)$$

$$I_n = \sqrt{\frac{it}{\pi}} \int_{\alpha}^{\beta} [a_n F_n(y) + b_n G_n(y)] e^{-it(y - x/M)^2} dy \quad (4.5b)$$

equation (4.4) becomes

$$v \left\{ 1 + \sum_{n=1}^N [a_n F_n(x) + b_n G_n(x)] \right\} = \sum_{n=0}^N I_n \quad (4.6)$$

The problem is to now apply the stationary phase approximation to the individual I_n 's and then sum the results. Starting with I_0 and comparing with equation (1.7), it is seen that

$$q(y) = \sqrt{\frac{it}{\pi}} \quad (4.7a)$$

and

$$p(y) = (y - x/M)^2 \quad (4.7b)$$

Also, from the stationary phase point definition, equation (1.9),

$$y_0 = x/M \quad (4.8)$$

Employing equation (1.8) and with some manipulation, it can be shown that

$$I_0 = 1 - \sqrt{\frac{1}{4i\pi t}} \left[\frac{e^{-it(\beta - x/M)^2}}{\beta - x/M} - \frac{e^{-it(\alpha - x/M)^2}}{\alpha - x/M} \right] \quad (4.9)$$

When written in terms of F_n and G_n from equation (3.11), this becomes

$$I_0 = 1 + F_1(x) + G_1(x) \quad (4.10)$$

Applying the same technique to I_1 , where

$$I_1 = \sqrt{\frac{it}{\pi}} \int_{\alpha}^{\beta} [a_1 F_1(y) + b_1 G_1(y)] e^{-it(y - x/M)^2} dy \quad (4.11)$$

the approximation yields

$$I_1 = a_1 F_2(x) + b_1 G_2(x) + F_1(x)[a_1 F_1(\beta) + b_1 G_1(\beta)] \\ + G_1(x)[a_1 F_1(\alpha) + b_1 G_1(\alpha)] \quad (4.12)$$

One more iteration is necessary in order to show a general trend. Again, using the stationary phase approximation to evaluate I_2 , the result is

$$I_2 = a_2 F_3(x) + b_2 G_3(x) + F_1(x)[a_2 F_2(\beta) + b_2 G_2(\beta)] \\ + G_1(x)[a_2 F_2(\alpha) + b_2 G_2(\alpha)] \quad (4.13)$$

From equations (4.10), (4.12), and (4.13) the resulting summation can be generalized to include all I_n 's, i.e.,

$$\sum_{n=0}^N I_n = 1 + F_1(x) + G_1(x) + \sum_{n=1}^N [a_n F_{n+1}(x) + b_n G_{n+1}(x)] \\ + F_1(x) \sum_{n=1}^N [a_n F_n(\beta) + b_n G_n(\beta)] \\ + G_1(x) \sum_{n=1}^N [a_n F_n(\alpha) + b_n G_n(\alpha)] \quad (4.14)$$

The equivalence of equations (4.6) and (4.14) gives rise to

$$v \{ 1 + \sum_{n=1}^N [a_n F_n(x) + b_n G_n(x)] \} = 1 + F_1(x) + G_1(x) \\ + \sum_{n=1}^N [a_n F_{n+1}(x) + b_n G_{n+1}(x)] \\ + F_1(x) \sum_{n=1}^N [a_n F_n(\beta) + b_n G_n(\beta)] + G_1(x) \sum_{n=1}^N [a_n F_n(\alpha) + b_n G_n(\alpha)] \quad (4.15)$$

The Polynomial Equation

From equation (4.15) a polynomial equation with determinable coefficients is developed. This eigenvalue polynomial (where v is the eigenvalue) is of order $2N + 1$ and is solved numerically. Each root is then associated with a different resonant mode of the cavity.

Referring to equation (4.15), the first step is to equate coefficients. For $n \neq 1$ we have

$$va_{n+1} = a_n = a_N v^{N-n} \quad (4.16a)$$

and

$$vb_{n+1} = b_n = b_N v^{N-n} \quad (4.16b)$$

Here the right equality is obtained from

$$a_{n+1} = \frac{a_n}{v} = \frac{a_1}{v^n} \quad (4.17)$$

and letting $n = N - 1$, i.e.,

$$a_N = \frac{a_1}{v^{N-1}} = \frac{a_n v^{n-1}}{v^{N-1}} = a_n v^{n-N} \quad (4.18)$$

The next step is to equate constant terms, which gives

$$v = 1 + a_N F_{N+1} + b_N G_{N+1} \quad (4.19)$$

Here the x dependence has been dropped since, by definition, the last functions to contribute to the spatial distribution of the field are $F_N(x)$ and $G_N(x)$, or that $F_{N+1}(x)$ and $G_{N+1}(x)$ are constant for all x .

Equating coefficients of $F_1(x)$ and $G_1(x)$ allows us to write

$$va_1 = 1 + \sum_{n=1}^N [a_n F_n(\beta) + b_n G_n(\beta)] \quad (4.20a)$$

and

$$vb_1 = 1 + \sum_{n=1}^N [a_n F_n(\alpha) + b_n G_n(\alpha)] \quad (4.20b)$$

Substitution for a_n , b_n , a_1 , and b_1 from equation (4.16) and rewriting equation (4.19) we obtain

$$a_N v^N = 1 + \sum v^{N-n} [a_n F_n(\beta) + b_n G_n(\beta)] \quad (4.21a)$$

$$b_N v^N = 1 + \sum v^{N-n} [a_n F_n(\alpha) + b_n G_n(\alpha)] \quad (4.21b)$$

$$v = 1 + a_N F_{N+1} + b_N G_{N+1} \quad (4.21c)$$

In the above equations the summations are understood to be from $n = 1$ to $n = N$. Although not readily apparent, equations (4.21) can be combined to yield a polynomial equation in v of order $2N + 1$. The expression is left to Appendix C, where it is seen that the coefficients are calculated from a knowledge of $F_n(\alpha)$, $F_n(\beta)$, $G_n(\alpha)$, $G_n(\beta)$, F_{N+1} , and G_{N+1} . Therefore, by specifying the quantities M , δ , and N_{eq} (refer to equations (3.9), (3.11), (3.12), and (4.3)), the roots of the polynomial are eventually determined.

Once the eigenvalues have been calculated, the constants a_n and b_n are determined for a particular mode (again refer to Appendix C). The resulting field is then evaluated at incremental positions across the feedback mirror, i.e.,

$$g(x) = 1 + \sum_{n=1}^N [a_n F_n(x) + b_n G_n(x)] \quad (4.22)$$

Given the field, $g(x)$, the phase is easily calculated from

$$\phi(x) = \arctan\left(\frac{y}{x}\right) \quad (4.23)$$

where $g(x)$ is the complex number $x + iy$.

Second Order Approximation

A higher order approximation to the method of stationary phase is required, due to the singularities involved, whenever y_0 approaches the endpoints of the integral. For I_0 (refer to equation (4.8)) and the case of a perfectly aligned resonator, this occurs when x approaches the shadow boundaries.

Since the v 's were determined from a valid first order approximation over the region $\alpha < x < \beta$, then the eigenvalues are acceptable for all x . This is justified by noting that v is a constant. The series constants a_n and b_n are also valid from the first approximation, refer to Appendix C, where it is seen that they are a function of the constants v^{N-n} , $F_n(\alpha)$, $G_n(\alpha)$, F_{N+1} , and G_{N+1} . This implies that in order to calculate the phase and intensity for all x values, a new approximation to the integral

$$I = \int_{\alpha}^{\beta} q(y) e^{-itp(y)} dy \quad (4.24)$$

is all that is required.

The higher order approximation to equation (4.24) can be simplified by letting

$$u(x) = e^{-itp(x)} q(x) \sqrt{\frac{\pi}{tp''(x)}} \exp\left[\frac{it[p'(x)]^2}{2p''(x)}\right] \quad (4.25a)$$

and

$$v(x) = \sqrt{\frac{t}{\pi p''(x)}} p'(x) \quad (4.25b)$$

Depending on the location of the stationary phase point, y_0 , the approximation takes one of three forms. They are: 1) for $y_0 \leq \alpha$

$$I = u(\beta) \left[E^*[v(\beta)] - \frac{1-i}{2} \right] - u(\alpha) \left[E^*[v(\alpha)] - \frac{1-i}{2} \right] \quad (4.26)$$

2) for $\alpha \leq y_0 \leq \beta$

$$I = e^{-i\pi/4} q(y_0) e^{-itp(y_0)} \sqrt{\frac{2\pi}{tp''(y_0)}} + u(\beta) \left[E^*[v(\beta)] - \frac{1-i}{2} \right] - u(\alpha) \left[E^*[v(\alpha)] + \frac{1-i}{2} \right] \quad (4.27)$$

and 3) for $y_0 \geq \beta$

$$I = u(\beta) \left[E^*[v(\beta)] + \frac{1-i}{2} \right] - u(\alpha) \left[E^*[v(\alpha)] + \frac{1-i}{2} \right] \quad (4.28)$$

(Ref. 3:29-30). In the above equations, E^* is the complex conjugate of the Fresnel integral.

Since the mathematics are again quite involved and tedious, the application of equations (4.26-4.28) will not be given. It is, however,

sufficient to say that the method of solution is similar to that of the first order approximation.

V. BEAM STEERING

The major effects of mirror misalignment in unstable resonators are beam steering and mode distortion. Mode distortion is easily verified by observation of the results presented in the next chapter. The geometrical beam steering angle, γ_g , is however not determined due to the mathematical construct of the misaligned resonator, i.e., the misaligned resonator is modeled as an aligned asymmetric resonator (see Figure 5-1). Additional information is required in order to calculate γ_g (refer to Chapter 3) since this analysis depends only on a knowledge of δ , M , and N_{eq} .

A diffracted beam steering angle, γ_d , is observed by comparison of Figures 6-2, 6-4, and 6-6. The phase fronts are seen to shift slightly with variations in the parameter δ . Since the normal to the phase front determines the direction of propagation, a straight line curve fit of the phase is desired.

This chapter calculates order of magnitude quantities for γ_g and θ (the mirror tilt angle). Also, a least squares curve fit is discussed for determination of γ_d .

Geometrical Beam Steering

The beam steering angle due to the geometric misalignment is the angle which the new optic axis makes with the old. From Figure 3-1

$$\gamma_g = \omega = \theta \frac{\xi_1 - 1}{1 - \xi_1 \xi_2} \quad (5.1)$$

Combining equations (3.8), (3.7), and (2.25) the tilt angle of the mirror

can be written as

$$\theta = \frac{a_2}{4Lg_1} \left[\frac{(M-1)^2}{M} \right] \delta \quad (5.2)$$

Substitution of equation (5.2) into (5.1) gives γ_g in terms of δ .

$$\gamma_g = \left[\frac{g_1 - 1}{1 - g_1 g_2} \right] \left[\frac{a_2}{4Lg_1} \right] \left[\frac{(M-1)^2}{M} \right] \delta \quad (5.3)$$

In order to make a comparative analysis later, we specify $M = 2.0$, $N_{eq} = 9.6$, and choose L to be 2.0 meters. From equations (B.6) and (2.25)

$$g_1 g_2 = \frac{1}{4}(M + 1/M + 2) = 1.125 \quad (5.4)$$

Calculating R_1 in terms of R_2 is possible by substitution of equation (1.1) in the above expression. The cavity configuration of Figure 5-1 is also desired (i.e., R_1 is positive and R_2 is negative), which gives

$$R_1 = \frac{L + R_2}{1 - (.125)N/L} \quad (5.5)$$

Having already specified R_1 as positive, requires

$$\frac{(0.125)R_2}{L} < 1.0 \quad (5.6)$$

or $R_2 < 16$ meters. Therefore, letting $R_2 = 10$ meters the value of R_1 is set at 32 meters. The maximum geometrical beam steering angle, γ_{gmax} , occurs for $\delta = 1.0$. For $\delta > 1$ there is no longer an axis within the

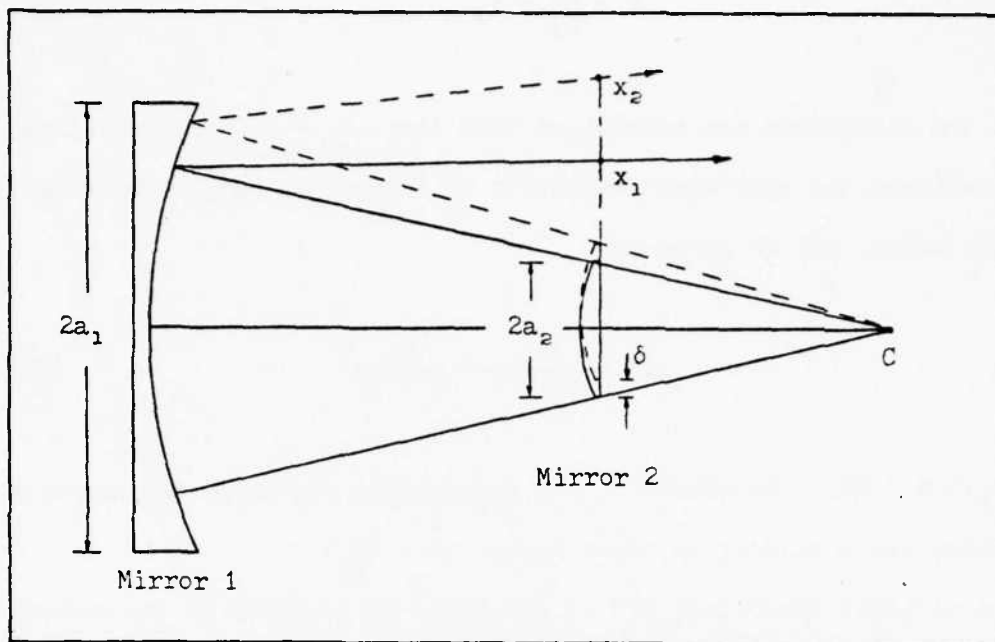


Fig. 5-1. The equivalent asymmetric cavity of the misaligned resonator as discussed in Chapter 3.

resonator with the symmetry of the original resonator, and there is no possibility of exciting modes characteristic of the aligned unstable resonator (Ref. 8:579-580). With $a_2 = 0.015$ meters, $\gamma_{g_{max}}$ is equal to 0.5 mrad. This is equivalent to a mirror tilt of approximately 1 mrad as calculated from equation (5.2).

Beam Steering Angles Due to Diffraction

The diffracted beam steering angle is first determined by finding the slope of the phase over the geometrical region. Referring to Figure 5-1, the region is seen to be from $-M+\delta M$ to $M+\delta M$. This is easily obtained by noting that the cavity magnification is a constant depending only on R_1 , R_2 , and L . The transverse magnification of the perfectly aligned resonator is defined as

$$M = \frac{x_1}{a_2} = x_1 \quad (5.7)$$

where the dimensions are normalized such that $a_2 = 1.0$. When mirror 2 is misaligned the equivalent resonator of Figure 5-1 has the same cavity magnification, and is given by

$$M = \frac{x_2}{a_2 + \delta} = \frac{x_2}{1 + \delta} \quad (5.8)$$

or $x_2 = M + \delta M$. The extent of the geometrical region in the negative direction can similarly be shown to be $-M + \delta M$.

A straight line curve fit of the phase is achieved by the method of least squares. Given n sets of points (x, y) , where y is the phase in radians and x is the normalized distance, the best straight line $y = mx + b$ is determined by solving the two normal equations

$$\begin{aligned} mn + m \sum x_j &= \sum y_j \\ b \sum x_j + m \sum x_j^2 &= \sum x_j y_j \end{aligned} \quad (5.9)$$

(Ref. 15:683), where the summation is from $j = 1$ to $j = n$. The diffracted beam steering angle is then

$$\tan \gamma_d \approx \gamma_d = \frac{d}{r} \quad (5.10)$$

The quantities d and r are the change in y and x respectively in MKS units, i.e., d is obtained from $e^{ikd} = e^{iy}$ and $r = a_2 x$. Therefore, the diffracted beam steering angle is

$$\gamma_d = \frac{\lambda y}{2\pi a_2 x} \quad (5.11)$$

From the results of the next chapter, the slope (y/x) is determined from the phase calculations for various values of δ and plotted in Figures 6-7 and 6-8. Analyzing the case of $M = 2$ and $N_{eq} = 9.6$ (Figure 6-7), $(y/x)_{max}$ is seen to be approximately 0.14. Also, from equations (2.28) and (2.25)

$$\frac{\lambda}{a_2} = \frac{a_2 (M - 1/M)}{4g_1 N_{eq} L} \quad (5.12)$$

which gives

$$\gamma_d = \frac{y}{x} \left[\frac{a_2 (M - 1/M)}{8\pi N_{eq} L g_1} \right] \quad (5.13)$$

Using the values from the previous cavity, $a_2 = 0.015$ m and $L = 2.0$ m, $\gamma_{d_{max}} \approx 7$ μ rad. The maximum value of 0.14 is seen to occur at $\delta = .225$, therefore; γ_g is equal to $0.225 \gamma_{g_{max}}$ or ≈ 0.1 mrad. It is clearly seen that the diffracted beam steering angle is approximately 7% of the geometrical beam steering angle, and is a significant contribution when considering propagation over long distances.

VI. Results, Conclusions

and

Recommendations

Results

The main result of this study is the development of the computer program, BARC 2, as listed in Appendix E along with a description of input variables. This code calculates intensity and phase in the plane of the feedback mirror by specifying δ , M , and N_{eq} . Also, the slope (y/x) is determined for the lowest loss mode only, where the diffracted beam steering angle is related to the slope by equation (5.13).

Plots of intensity and phase for the first three modes of a cavity with $M = 2.0$ and $N_{eq} = 9.6$ are at the end of this section and in Appendix D. For various δ , the intensity and phase distortion is clearly evident. The phase of the lowest loss mode (Figures 6-2, 6-4, and 6-6) is seen to remain relatively uniform, but has a definite slope or directionality associated with it as δ changes. This slope is plotted in Figure 6-7 for a range of δ between 0.0 and 0.25.

For the cavity configuration chosen in Chapter 5, the diffracted beam steering angle is a significant portion of the total beam steering angle for specific values of δ . Again referring to Figure 6-7, for $\delta = 0.01125$ the slope is 0.1304. This gives $\gamma_d \approx 6.5 \mu\text{rad}$ and $\gamma_g = 0.01125 \gamma_{Gmax} \approx 5.6 \mu\text{rad}$, which shows that γ_d is of the order of γ_g when $\delta \approx 0.01$. This value is, however, totally dependent on cavity geometry and must be evaluated for each resonator as discussed in Chapters 3 and 5. More importantly, γ_d is seen to vary with no apparent regularity as δ varies.

Conclusions

By comparison of the phase and intensity plots with those in Reference 5, the basic conclusion reached is that program BARC2 produces valid results. Also, for the case of a perfectly aligned resonator, i.e. $\delta = 0$, the results are consistent with those of the previous study (Ref. 3).

As shown in Chapter 3, the geometrical beam steering angle is a linear function of the mirror tilt angle for small misalignments. This has been confirmed from a previous analysis by Krupke and Sooy (Ref. 8). Also, the diffracted beam steering angle is of the order of the geometrical beam steering angle for $\delta \ll 1.0$; however the exact limit depends on which mirror is misaligned and the cavity geometry.

The irregularities associated with the diffracted beam steering angle versus mirror misalignment (Figures 6-7 and 6-8) is a result of the structure in the phase. Had the feedback mirror been illuminated by a plane wave of infinite extent, the diffracted beam steering angle would have been zero for all δ since the mathematical model is simply a translation of the diffracting obstacle (see Figure 5-1). Referring to Figure 6-2, when the mirror is translated to the right (the dashed lines indicate the position of the mirror) it intercepts a further advanced wave on the right than on the left, and a definite slope is observed in the phase front. Specifically, at $\delta \approx 0.2$ (again refer to Figure 6-2) the extent of the mirror becomes -0.8 to 1.2 where a peak in the phase is intercepted on the right and a minimum on the left. This produces the maximum beam steering angle of Figure 6-7.

Further inspection of Figure 6-2 would require $\gamma_{d_{\max}}$ to occur at $\delta \approx 0.9$. This is exactly the case and the slope at this point is 0.519. The reason for terminating the plots in Figures 6-7 and 6-8 at $\delta = 0.25$

is due to the excessive amount of computer time required to generate them. Therefore, relative values for the diffraction beam steering angle can be estimated from the phase of the perfectly aligned resonator.

Recommendations

The computer model, developed from the previous analysis, calculates intensity and phase in the plane of the feedback mirror for the case of a bare strip resonator. A beam steering angle due to diffraction is also determined for the lowest loss mode.

An obvious extension would be to determine beam steering angles for all possible modes of the cavity. In addition, the model might be modified to account for the presence of a saturated or non-uniform gain medium. Since the analysis was restricted to mirrors with rectangular apertures, the case of circular mirrors would be another topic for investigation.

Still another area of consideration would be the analysis of mirror tilt and its effect on higher order aberrations; or the change in the phase slope vs. mirror misalignment curves for higher Fresnel numbers.

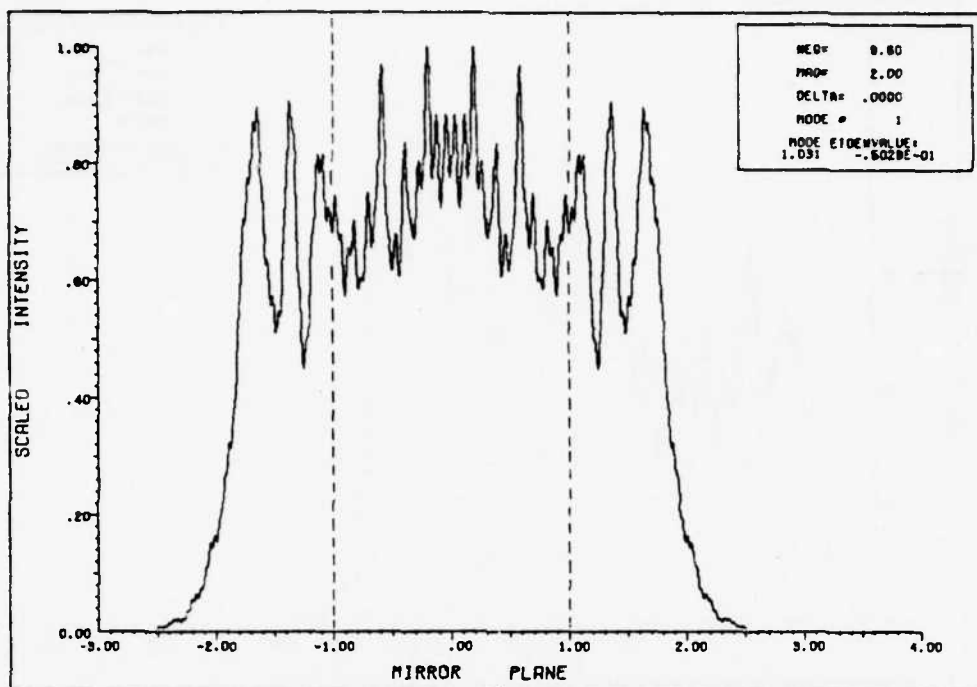


Fig. 6-1. Intensity plot for the lowest loss mode with $\delta = 0.0$.

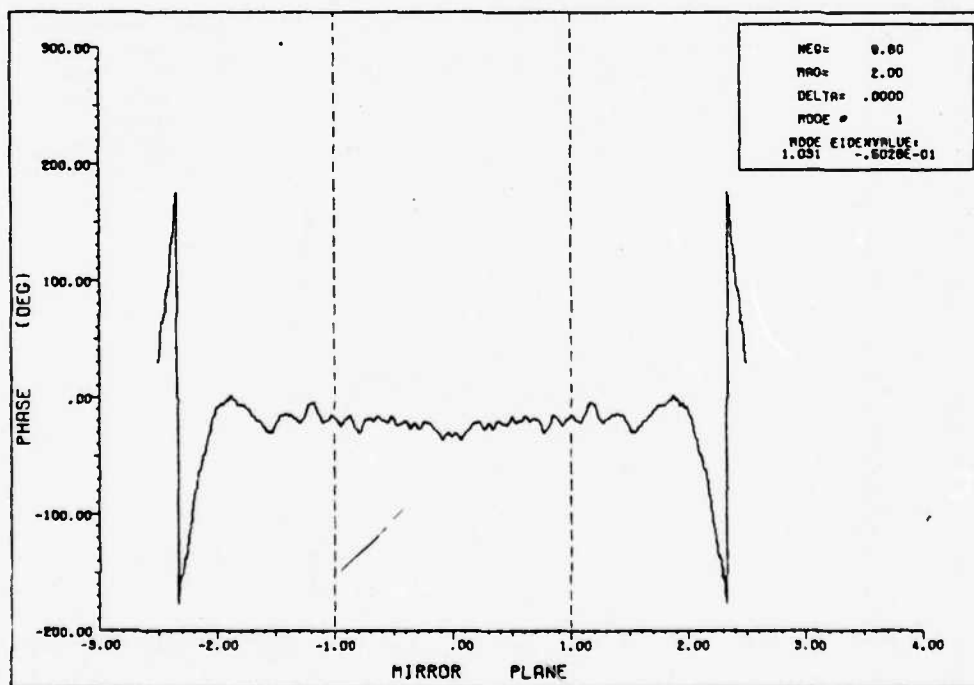


Fig. 6-2. Phase plot for the lowest loss mode with $\delta = 0.0$.

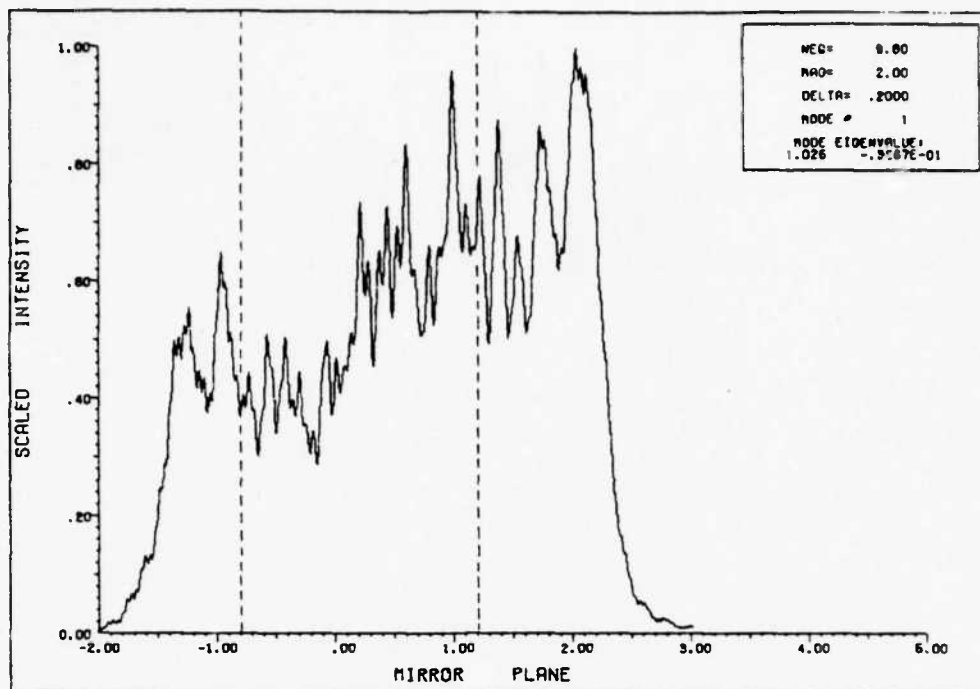


Fig. 6-3. Intensity plot for the lowest loss mode with $\delta = 0.2$.

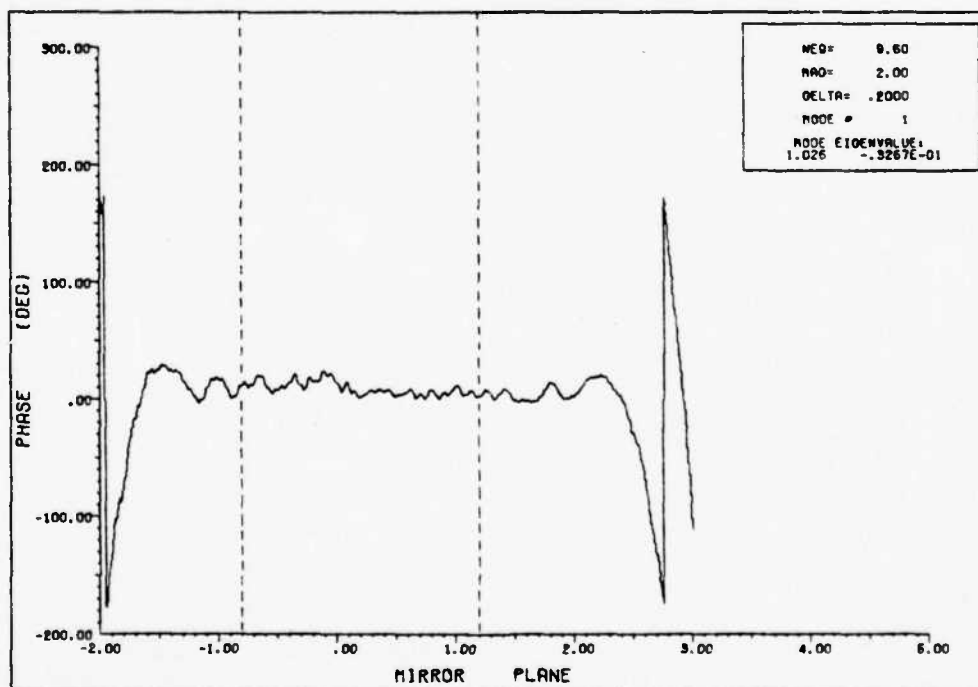


Fig. 6-4. Phase plot for the lowest loss mode with $\delta = 0.2$.

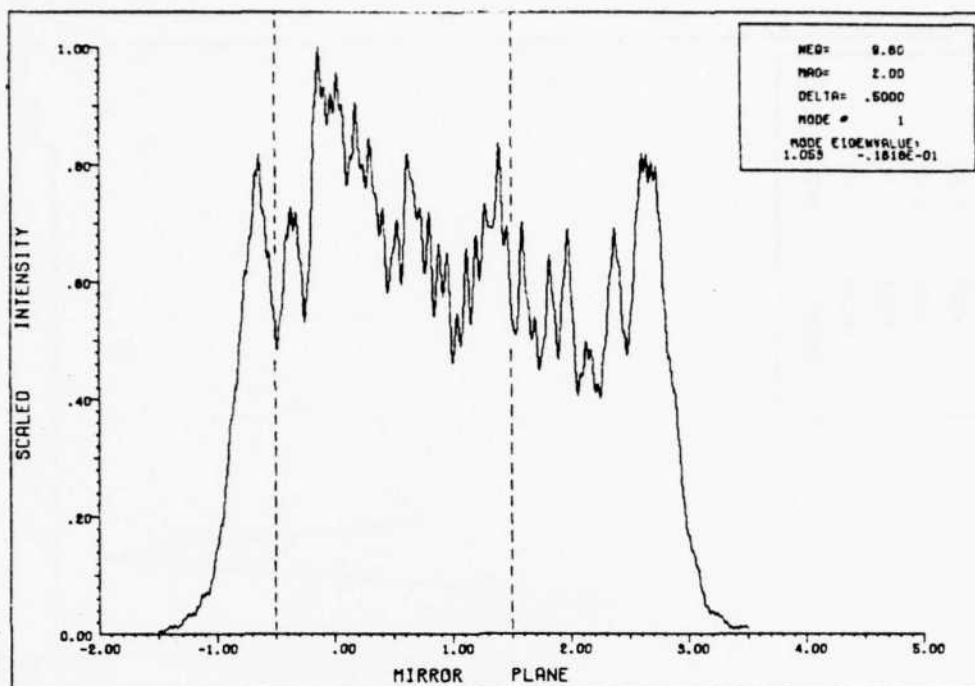


Fig. 6-5. Intensity plot for the lowest loss mode with $\delta = 0.5$.

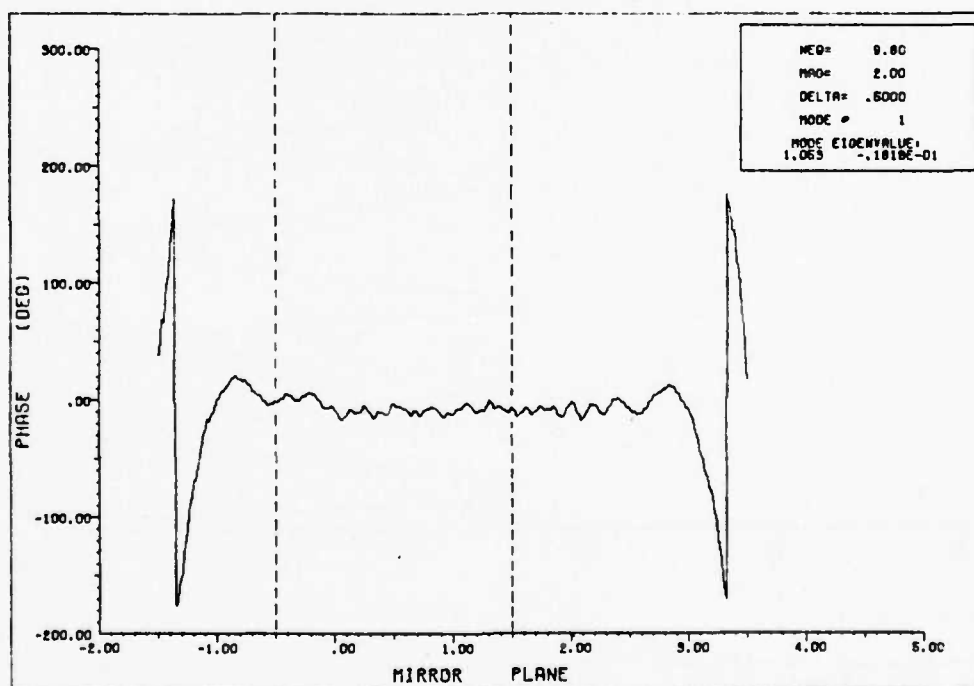


Fig. 6-6. Phase plot for the lowest loss mode with $\delta = 0.5$.

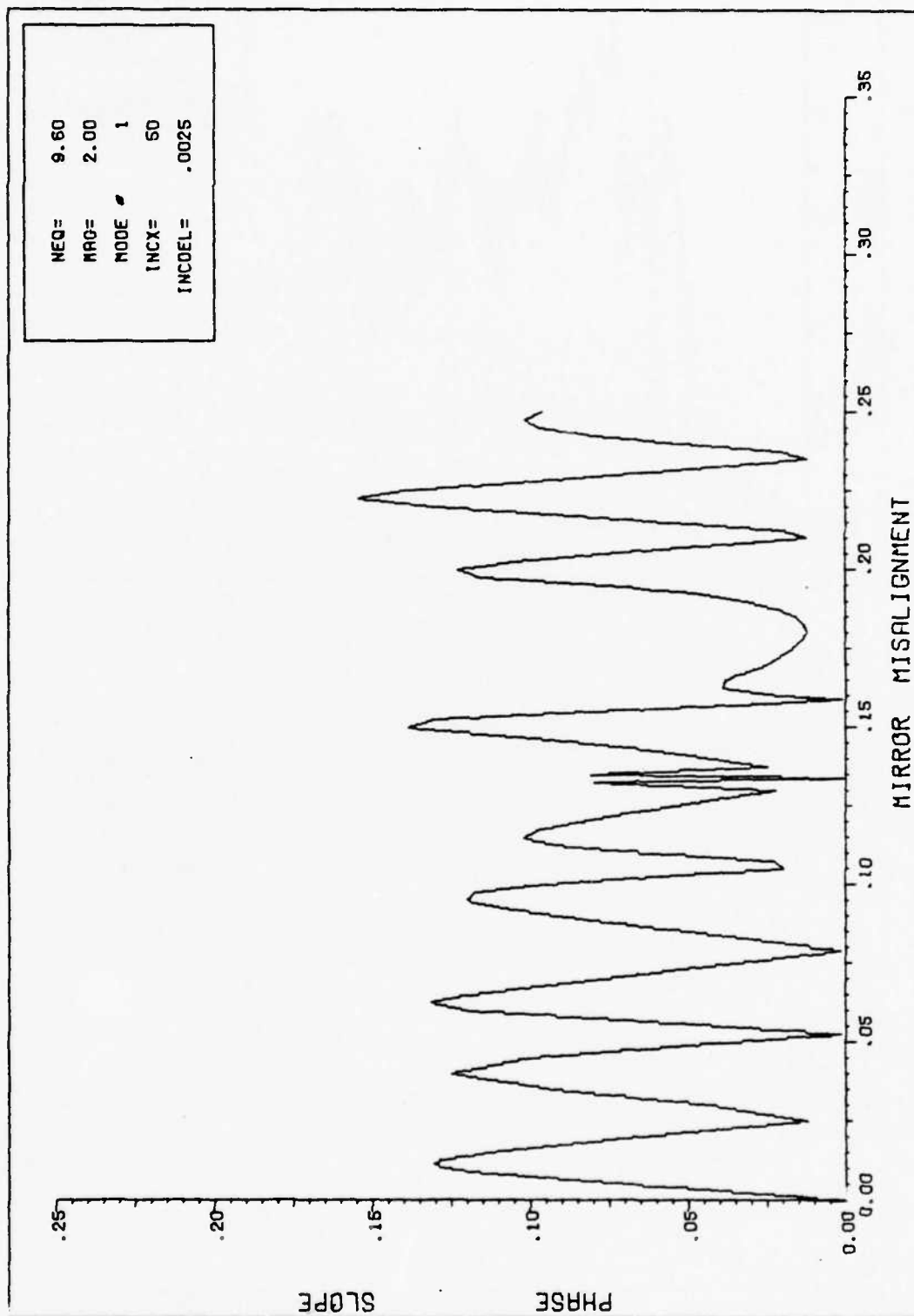


Fig. 6-7. Phase slope vs. mirror misalignment, δ . INCDEL is the increment value of δ for which the slope was calculated.

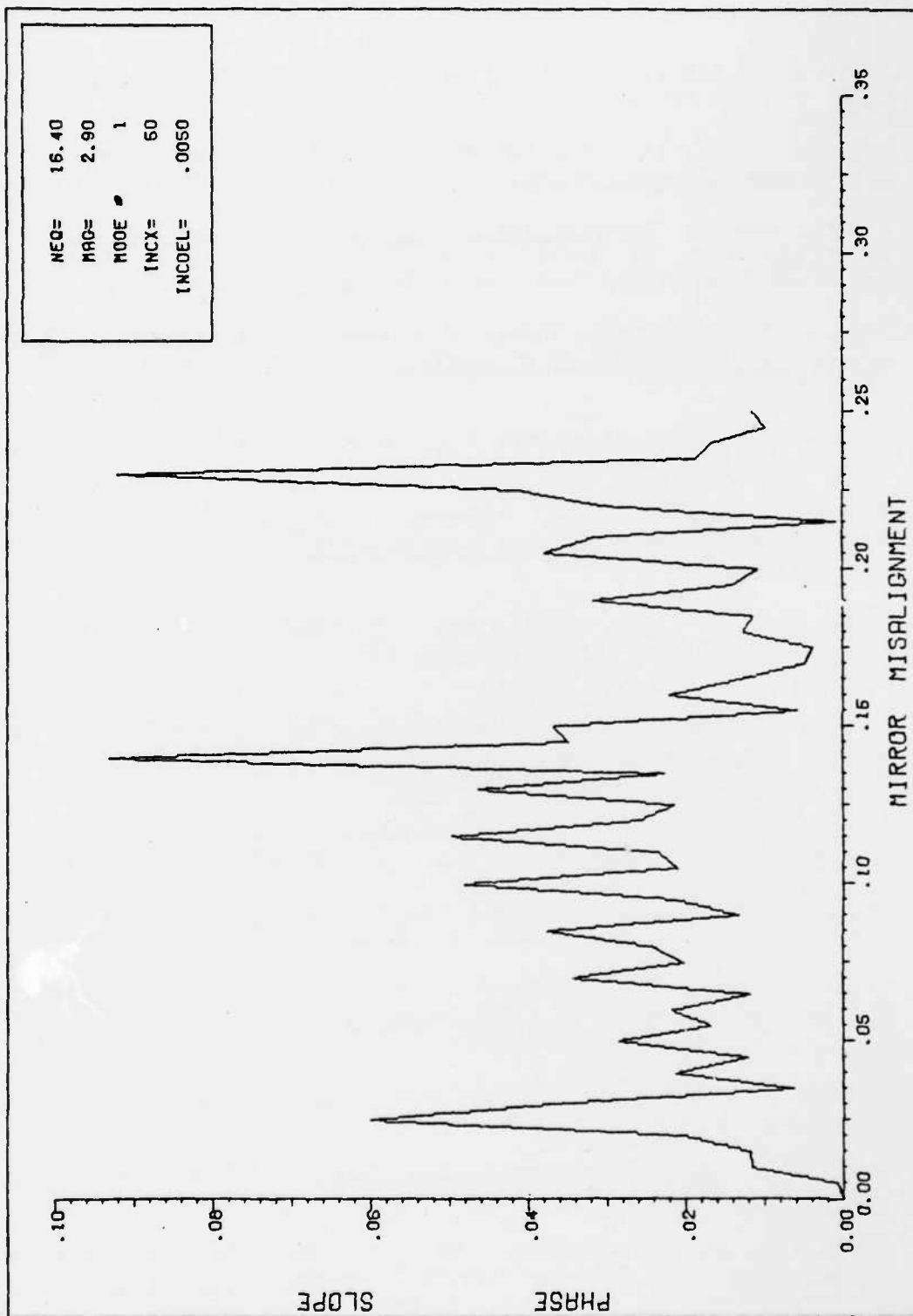


Fig. 6-8. Phase slope vs. mirror misalignment, δ . INCDEL is the increment value of δ for which the slope was calculated.

BIBLIOGRAPHY

1. Kogelnik, H. and T. Li. "Laser Beams and Resonators," Proceedings IEEE, Vol. 54, No. 10: 1312-1329 (Oct. 1966).
2. Fox, A.G. and T. Li. "Resonant Modes in a Maser Interferometer," Bell System Technical Journal, Vol. 40, No. 2: 453-488 (March 1961).
3. Rowley, James E. Computer Analysis of Modes in an Unstable Strip Laser Resonator. MS Thesis. Wright-Patterson AFB, Ohio: School of Engineering, Air Force Institute of Technology, Dec. 1980.
4. Horwitz, P. "Asymptotic Theory of Unstable Resonator Modes," Journal of the Optical Society of America, Vol. 63, No. 12: 1528-1543 (Dec. 1973).
5. -----, "Modes in Misaligned Unstable Resonators," Applied Optics, Vol. 15, No. 1: 167-178 (Jan. 1976).
6. Perkins, J.F. and C. Cason. "Effects of Small Misalignments in Empty Unstable Resonators," Applied Physics Letters, Vol. 31, No. 3: 198-200 (Aug. 1977).
7. Hauck, R., H.P. Kortz, and H. Weber. "Misalignment Sensitivity of Optical Resonators," Applied Optics, Vol. 19, No. 4: 598-601 (Feb. 1980).
8. Krupke, W.F. and W.R. Sooy. "Properties of an Unstable Confocal Resonator CO₂ Laser System," IEEE Journal of Quantum Electronics, Vol. QE-5, No. 12: 575-586 (Dec. 1969).
9. Siegman, A.E. "Unstable Optical Resonators for Laser Applications," Proceedings of the IEEE, Vol. 53, No. 3: 277-287 (March 1965).
10. Sanderson, R.L. and W. Streifer. "Laser Resonators with Tilted Reflectors," Applied Optics, Vol. 8, No. 11: 2241-2248 (Nov. 1969).
11. Siegman, A.E. and R. Arrathoon. "Modes in Unstable Optical Resonators and Lens Waveguides," IEEE Journal of Quantum Electronics, Vol. QE-3, No. 4: 156-163 (April 1967).
12. Siegman, A.E. "Unstable Optical Resonators," Applied Optics, Vol. 13, No. 2: 353-367 (Feb. 1974).
13. Beyer, W.H. CRC Standard Mathematical Tables (25th Edition). Boca Raton, Florida: CRC Press, Inc., 1980.
14. Butts, R.R. and P.V. Avizonis. "Asymptotic Analysis of Unstable Laser Resonators with Circular Mirrors," Journal of the Optical Society of America, Vol. 68, No. 8: 1072-1078 (Aug. 1978).

15. Kreyszig, E. Advanced Engineering Mathematics (3rd Edition). New York: John Wiley and Sons, Inc., 1972.

APPENDIX A

Appendix A is devoted to the evaluation of the definite integral in equation (2.23).

$$\frac{i}{\lambda L} \int_{-\infty}^{\infty} e^{-\frac{ik}{2L}(x_1^2 \epsilon_1 + x^2 \epsilon_2 - 2x_1 x)} e^{-\frac{ik}{2L}(x_1^2 \epsilon_1 + y^2 \epsilon_2 - 2x_1 y)} dx_1 \quad (A.1)$$

The exponentials can be combined to yield

$$\frac{i}{\lambda L} e^{-\frac{ik}{2L} \epsilon_2 (x^2 + y^2)} \int_{-\infty}^{\infty} e^{-\frac{ik}{2L} [2x_1^2 \epsilon_1 - 2x_1 (x + y)]} dx_1 \quad (A.2)$$

Completing the square in the exponent, the integral becomes

$$\frac{i}{\lambda L} e^{-\frac{ik}{2L} \epsilon_2 (x^2 + y^2)} e^{\frac{ik(x+y)^2}{4L\epsilon_1}} \int_{-\infty}^{\infty} e^{-\frac{ik}{L} [x_1^2 \epsilon_1 - x_1 (x + y) + \frac{(x + y)^2}{4\epsilon_1}]} dx_1 \quad (A.3)$$

Instead of (A.3), we write the integral as

$$\frac{i}{\lambda L} \exp\left[-\frac{ik}{2L} \epsilon_2 (x^2 + y^2) - \frac{(x + y)^2}{2\epsilon_1}\right] \int_{-\infty}^{\infty} \exp\left[-\frac{ik}{L} \left[x_1 \sqrt{\epsilon_1} - \frac{x + y}{2\sqrt{\epsilon_1}}\right]^2\right] dx_1 \quad (A.4)$$

Now, if we let

$$\beta = \frac{k}{L} = \frac{2\pi}{\lambda L} \quad (A.5)$$

and

$$v = \left(x_1 \sqrt{\epsilon_1} - \frac{x + y}{2\sqrt{\epsilon_1}}\right)$$

then the resulting integral is

$$\int_{-\infty}^{\infty} \frac{e^{-i\beta V^2}}{\sqrt{\epsilon_1}} dV \quad (A.6)$$

where the constant term in front of (A.4) has been dropped. With the additional definitions

$$\begin{aligned} \omega &= \sqrt{\beta} V \\ d\omega &= \sqrt{\beta} dV \end{aligned} \quad (A.7)$$

the definite integral of (A.6) is written

$$\int_{-\infty}^{\infty} \frac{e^{-i\omega^2}}{\sqrt{\beta\epsilon_1}} d\omega = \frac{2}{\sqrt{\beta\epsilon_1}} \int_0^{\infty} e^{-i\omega^2} d\omega = \sqrt{\frac{\pi}{i\beta\epsilon_1}} \quad (A.8)$$

(Ref. 13:380); evaluation of the integral can be found in any handbook of mathematics. Substituting the value of β , from (A.5), into (A.8) yields the constant

$$\sqrt{\frac{L\lambda}{2i\epsilon_1}} \quad (A.9)$$

With the integral evaluated, (A.4) becomes

$$\sqrt{\frac{i}{2\lambda L\epsilon_1}} \exp\left[-\frac{ik_r}{2L}\epsilon_2(x^2 + y^2) - \frac{(x+y)^2}{2\epsilon_1}\right] \quad (A.10)$$

If the exponential is expanded with a common denominator of $4L\epsilon_1$, then

(A.10) takes the final form of the kernel when the substitution of $2\pi/\lambda$ is made for k , i.e.,

$$\sqrt{\frac{i}{2\lambda L g_1}} \exp\left[-\frac{i\pi}{2\lambda L g_1} [(2g_1 g_2 - 1)(x^2 + y^2) - 2xy]\right] \quad (\text{A.11})$$

APPENDIX B

Before equation (2.31) takes the form of equation (1.3), substitution of some variables must be accomplished.

$$\gamma g(x) e^{-\frac{i\pi F}{2}(M - \frac{1}{M})x^2} = \sqrt{iF} \int_{-1}^1 g(y) e^{-\frac{i\pi F}{2}(M - \frac{1}{M})y^2} e^{-i\pi F[g(x^2 + y^2) - 2xy]} dy \quad (B.1)$$

Given

$$M = \frac{\sqrt{g+1} + \sqrt{g-1}}{\sqrt{g+1} - \sqrt{g-1}} \quad (B.2)$$

(Ref. 11:157) and solving for g , we get

$$M = \frac{(\sqrt{g+1} + \sqrt{g-1})^2}{g+1 - (g-1)} \quad (B.3)$$

$$M = g + \sqrt{g^2 - 1} \quad (B.4)$$

$$(M - g)^2 = g^2 - 1 \quad (B.5)$$

$$g = \frac{M^2 + 1}{2M} \quad (B.6)$$

Substitution of this in equation (B.1), the integral becomes

$$\gamma g(x) = \sqrt{iF} \int_{-1}^1 g(y) e^{-\frac{i\pi F}{2}[(M - \frac{1}{M})(y^2 - x^2) + (x^2 + y^2)(M + \frac{1}{M}) - 4xy]} dy \quad (B.7)$$

$$\gamma g(x) = \sqrt{iF} \int_{-1}^1 g(y) e^{-i\pi F(\frac{x^2}{M} + My^2 - 2xy)} dy \quad (B.8)$$

$$\gamma g(x) = \sqrt{iF} \int_{-1}^1 g(y) e^{-i\pi MF(y - x/M)^2} dy \quad (B.9)$$

If we define

$$t = \pi MF \quad (B.10)$$

then equation (B.9) can be written

$$\gamma g(x) = \sqrt{\frac{it}{\pi M}} \int_{-1}^1 g(y) e^{-it(y - x/M)^2} dy \quad (B.11)$$

Letting

$$v = \gamma\sqrt{M} \quad (B.12)$$

equation (1.3) is arrived at, i.e.,

$$v g(x) = \sqrt{\frac{it}{\pi}} \int_{-1}^1 g(y) e^{-it(y - x/M)^2} dy \quad (B.13)$$

APPENDIX C

The coefficients of the polynomial are not readily determined from the form listed below; however, with the following definitions it is the most concise form available.

$$\begin{aligned}
 F_{\alpha} &= \sum v^{N-n} F_n(\alpha) \\
 F_{\beta} &= \sum v^{N-n} F_n(\beta) \\
 G_{\alpha} &= \sum v^{N-n} G_n(\alpha) \\
 G_{\beta} &= \sum v^{N-n} G_n(\beta)
 \end{aligned}
 \tag{C.1}$$

Here it is understood that the summation is from $n = 1$ to $n = N$. The polynomial is now written as

$$\begin{aligned}
 &v^{2N+1} - v^{2N} - v^{N+1}(F_{\beta} + G_{\alpha}) + v^N(F_{\beta} - F_{N+1} + G_{\alpha} - G_{N+1}) \\
 &+ v(F_{\beta}G_{\alpha} - F_{\alpha}G_{\beta}) + (F_{\alpha}G_{\beta} - F_{\beta}G_{\alpha}) \\
 &+ F_{N+1}(G_{\alpha} - G_{\beta}) - G_{N+1}(F_{\alpha} - F_{\beta}) = 0
 \end{aligned}
 \tag{C.2}$$

Also, the F_{N+1} and G_{N+1} are the series functions with the x dependence neglected.

The constants a_n and b_n are then calculated, once the eigenvalues have been determined, by specifying a particular mode. The first two equations of (4.21) are combined to yield

$$b_N = \frac{1 + \frac{\nu-1}{F_{N+1}} \sum \nu^{N-n} F_n(\alpha)}{\nu^N - \sum \nu^{N-n} G_n(\alpha) + \frac{G_{N+1}}{F_{N+1}} \sum \nu^{N-n} F_n(\alpha)} \quad (C.3)$$

Here again the summation is from $n = 1$ to $n = N$.

The a_N 's and b_N 's are coupled through the third equation of (4.21), and from equations (4.16) the resulting series constants are determined, i.e.,

$$b_n = b_N \nu^{N-n}$$

$$a_n = \frac{\nu^{N-n}(\nu-1) - b_n G_{N+1}}{F_{N+1}} \quad (C.4)$$

APPENDIX D

The plots presented here are a few of the higher loss modes, and are included for additional verification of the computer program by comparison with the graphs found in Reference 5. All but the last two plots are a result of the second order approximation. Figures D-9 and D-10 are seen to be the intensity and phase across the feedback mirror only, and are identical in structure to Figures 6-1 and 6-2.

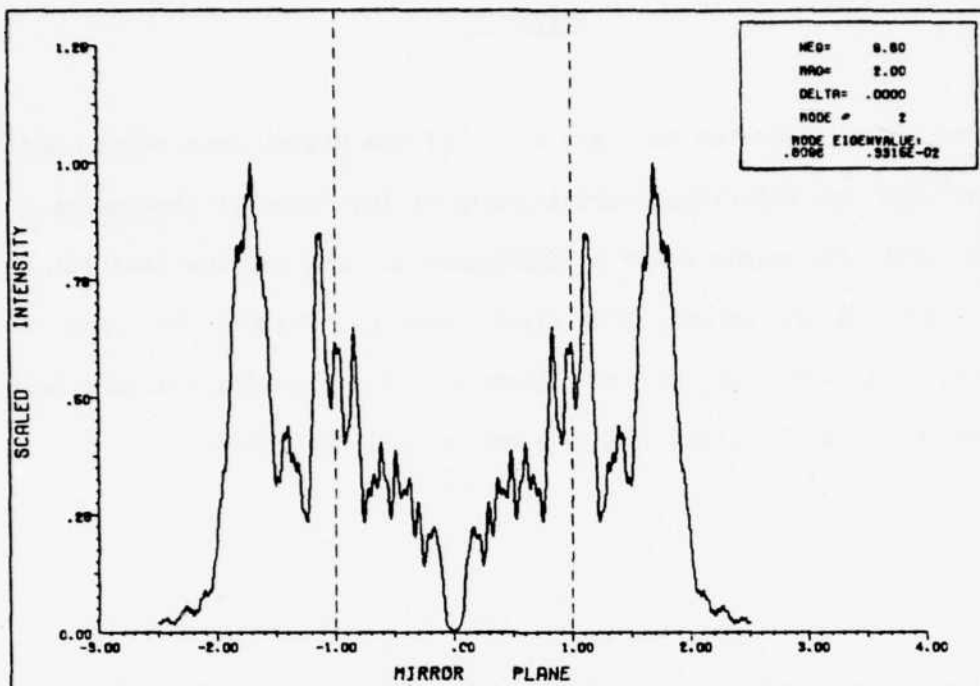


Fig. D-1. Intensity plot for mode #2 .

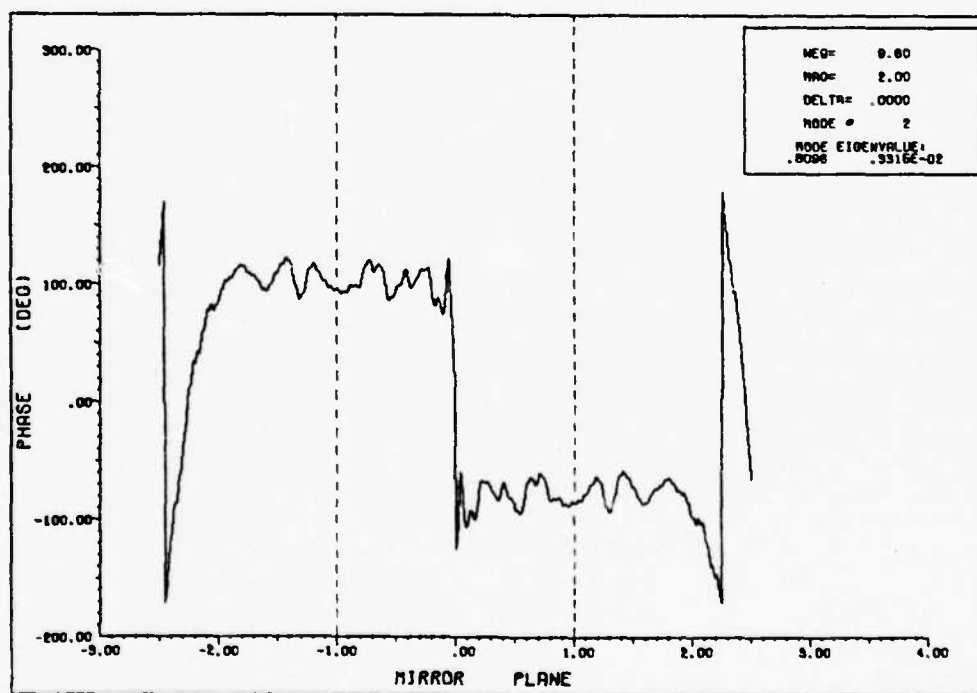


Fig. D-2. Phase plot for mode #2 .

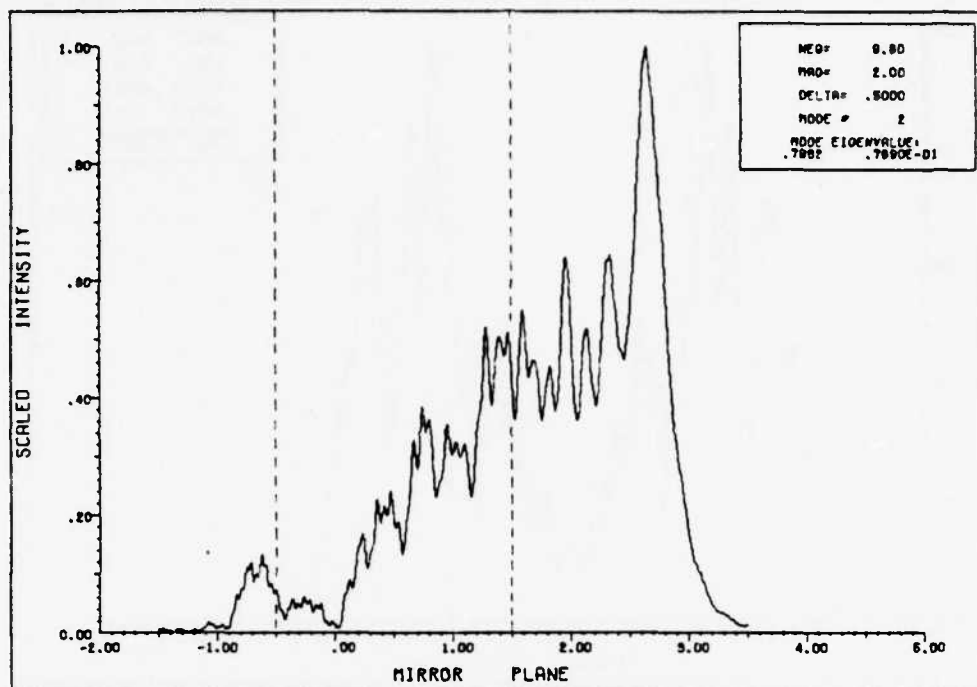


Fig. D-3. Intensity plot for mode #2 and $\delta = 0.5$.

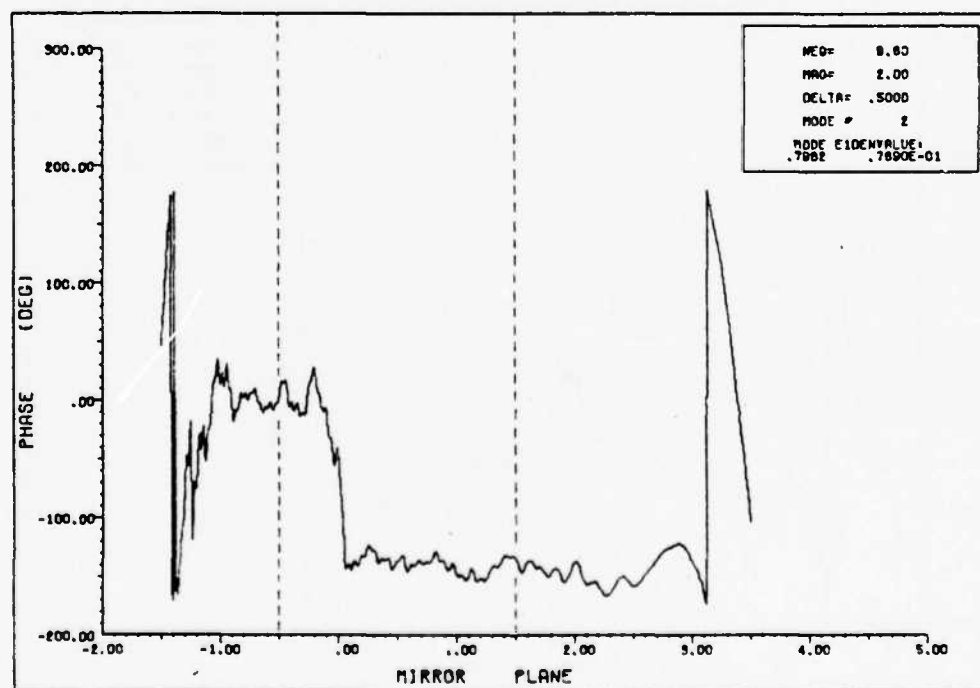


Fig. D-4. Phase plot for mode #2 and $\delta = 0.5$.

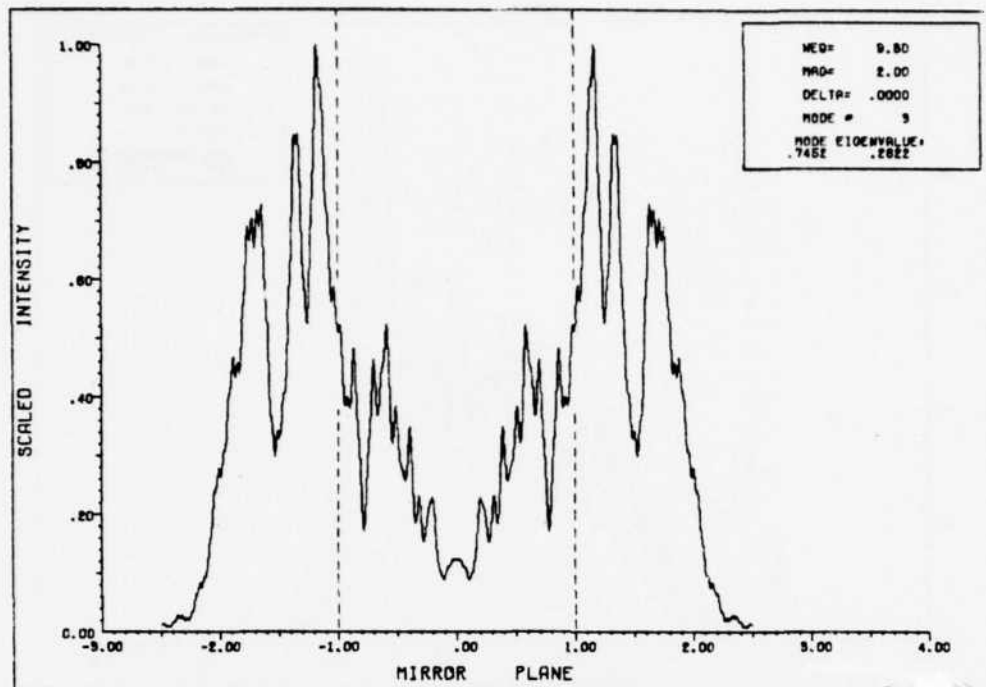


Fig.D-5. Intensity plot for mode #3 and $\delta = 0.0$.

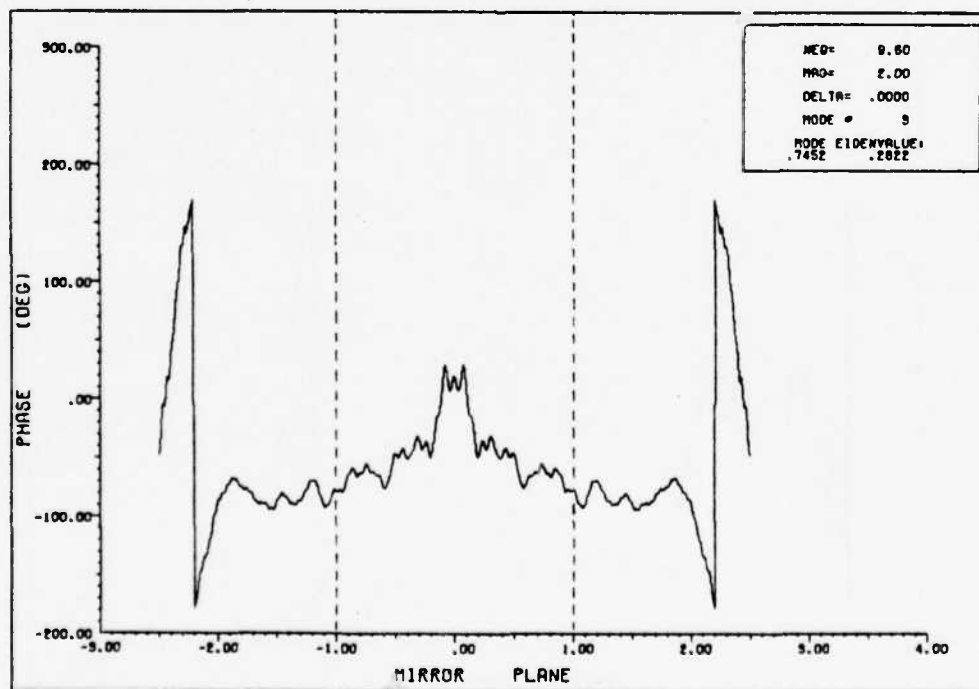


Fig. D-6. Phase plot for mode #3 and $\delta = 0.0$.

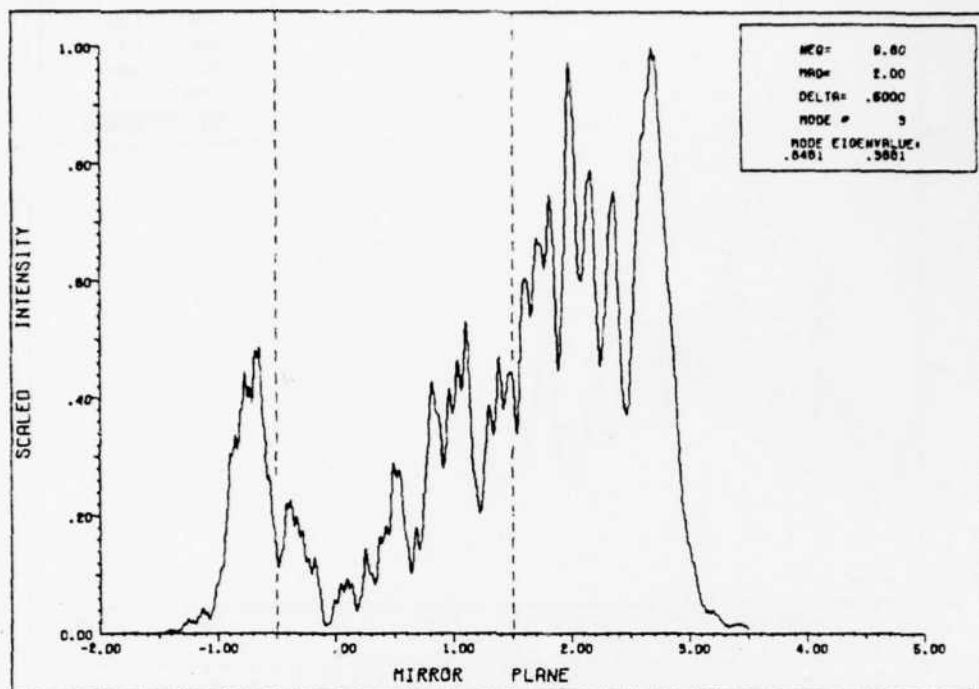


Fig. D-7. Intensity plot for mode #3 and $\delta = 0.5$.

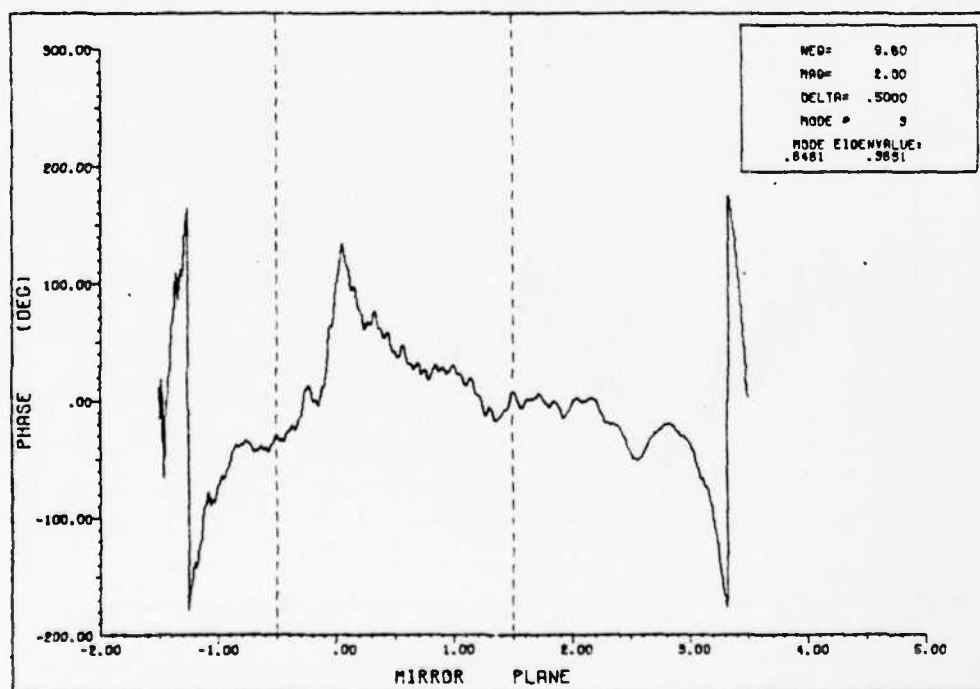


Fig. D-8. Phase plot for mode #3 and $\delta = 0.5$.

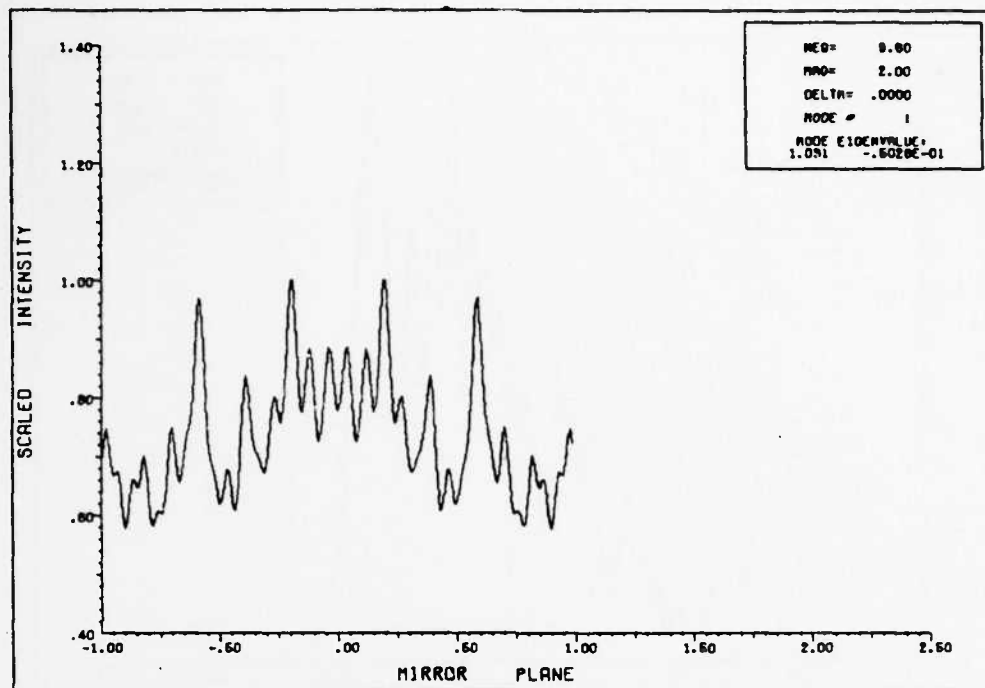


Fig. D-9. Intensity plot across the feedback mirror only using the first order approximation.

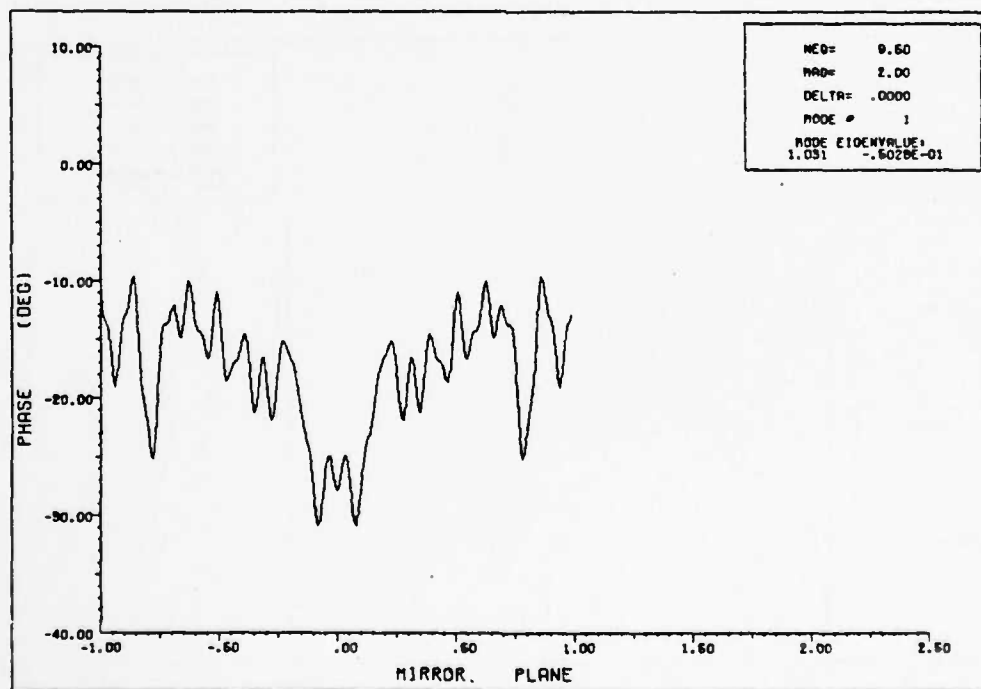


Fig. D-10. Phase plot across the feedback mirror only using the first order approximation.

APPENDIX E

A listing of program BARC2 employing the analysis and derivations of the preceding chapters is given here. Also included is a list of input variables required for program operation. Unless otherwise stated, the input variables follow normal Fortran convention for being either real or integer values.

BARC2 Inputs (variables are listed in order required) -

- MAG: Cavity magnification (real)
- NEQ: Equivalent Fresnel number (real)
- DELTA: Mirror misalignment (offset in fraction of mirror radius)
- NBIG: Desired number of terms in field series
- MTEST1: Input 0 to list eigenvalues.
- MTEST2: Input 0 to continue with other options, 1 to do new cavity (MAG,NEQ,DELTA), or 2 to exit.
- MODE: Desired mode number for phase and intensity calculations (1 to $2 \cdot \text{NBIG} + 1$). The eigenvalues, λ , are listed according to loss, i.e., mode #1 is the lowest loss mode.
- MTEST3: Input 0 to calculate intensity and phase, 1 to continue with other options, or 2 to exit.
- MTEST4: Input 0 to calculate intensity over expanded range. If MTEST4 equals 0, control is to subroutine ALLINT with variables INCX and MTEST5 skipped.
- INCX: Increment value of x for phase and intensity calculation
- MTEST5: Input 0 to list field, phase, and intensity across the feedback mirror.
- MTEST6: Input 0 to plot constants a_n and b_n versus NBIG, 1 to return, or 2 to exit (return is to MTEST2). If MTEST6 equals 0, the plots are generated and control is automatically returned to MTEST2.

Note - INCX is the integer number of points between consecutive whole x values. For example, INCX = 100 specifies 100 points between $x = 0$ and $x = 1$ for the phase and intensity calculations.

Subroutine ALLINT Inputs -

XMIN: Minimum x value over which intensity and phase are calculated.

XMAX: Maximum x value over which intensity and phase are calculated.

INCX: Increment value of x

NTEST1: Input 0 to list field, phase, and intensity.

NTEST2: Input 0 to plot intensity and phase.

Program operation is returned to MTEST6 in BARC2.

Note - For the best results let: $XMIN = -MAG + DELTA * MAG - 0.5$

and $XMAX = +MAG + DELTA * MAG + 0.5$

- Since ZCPOLY (the root finding routine) limits the degree of the polynomial to 49, the maximum value for NBIG is 24 .

```

100=      PROGRAM BARC2(DATA,INPUT,OUTPUT,TAPE8=OUTPUT,TAPE4=DATA)
110=      COMMON STOREX(700),PHASE(700),XINTEN(700),PHASE2(700)
120=      REAL NEQ,MAG,MSURN(51),MSUPN(51)
130=      COMPLEX EYE,COEF(51),LAMBDA(51),CONSTA(51),FIELD(700)
140=      COMPLEX CL(51),CDUM,AN1,AN2,X1,X2,Y1,Y2,Z1,Z2
150=      COMPLEX ROOT,CONSTR(51),PCONA(51),PCUNE(51),FNX,GNX
160=      COMPLEX FBETA(51),FALPHA(51),GBETA(51),GALPHA(51)
170=      DIMENSION RINDEX(51),LABEL(25)
180=      DATA LABEL/25(10H          )//
190=C*****
200=C
210=C      THIS PROGRAM COMPUTES RESONATOR MODE EIGENVALUES AND
220=C      SUBSEQUENTLY EVALUATES INTENSITY VALUES FOR POINTS
230=C      ACROSS THE OUTPUT PLANE OF A STRIP LASER RESONATOR.
240=C      THE PROGRAM DEALS ONLY WITH A BARE CAVITY.
250=C      OUTPUT CONSISTS OF AN EIGENVALUE LIST, WITH PHASE
260=C      AND MAGNITUDE, FIELD VALUES FOR A SELECTED MODE
270=C      EITHER ON OR OFF THE MIRROR, PLOTS OF FIELD SERIES
280=C      FUNCTIONS OR WEIGHTING CONSTANTS, AND PLOTS OF INTENSITY
290=C      ACROSS THE OUTPUT PLANE WITH EITHER LIMITED OR EXTENDED
300=C      RANGE.
310=C      COMPILED CODE NEEDED AROUND 110000 OCTAL TO LOAD.
320=C
330=C      INPUT QUANTITIES ARE AS FOLLOWS:
340=C      DELTA = MIRROR MISALIGNMENT (OFFSET IN FRACTION OF MIRROR RADIUS)
350=C      MAG = CAVITY MAGNIFICATION
360=C      NEQ = EQUIVALENT FRESNEL NUMBER
370=C      RNBIG = DESIRED # TERMS IN FIELD SERIES
380=C
390=C      NOTE: EVMAG DENOTES EIGENVALUE MAGNITUDE, AND EUPH DENOTES
400=C      EIGENVALUE PHASE.
410=C      THIS PROGRAM ALSO REQUIRES IMSL ROUTINE ZCPOLY AND PLOTTING
420=C      ROUTINE DCPLOTS6X. FINAL COPY, 20 SEPT 1981. R W BERDINE
430=C
440=C*****
450=      PI=2.*ASIN(1.0)
460=      EYE=CMPLX(0.,1.)
470=994    FORMAT(F6.2,4X)
480=990    FORMAT(1X,F5.4,4X)
490=      LABEL(1)=10H    NEQ=
500=      LABEL(3)=10H    MAG=
510=      LABEL(13)=10H   DELTA=
520=777    WRITE(8,999)
530=999    FORMAT(1H1,1X,*INPUT MAG, NEQ, AND OFFSET: *,/)
540=      READ *,MAG,NEQ,DELTA
550=      WRITE(8,88)MAG,NEQ,DELTA
560=      WRITE(4)MAG,NEQ,DELTA
570=      LABEL(5)=10H   MODE EIG
580=      LABEL(6)=10HEIGENVALUE:
590=C*****
600=C
610=C      MSUPN(I)=MAG**(I-1)
620=C      MSURN(I)=1+1/MAG**2 + ... +1/MAG**(2*I-2)
630=C
640=C*****
650=      MSURN(1)=1.0
660=      MSUPN(1)=1.0
670=      DO 10 I=2,51
680=      MSUPN(I)=MAG*MSUPN(I-1)
690=      MSURN(I)=MSURN(I-1)+1./MSUPN(I)**2
700=10      CONTINUE
710=      I=2*NEQ*PI*MAG**2/(MAG**2-1.)
720=      RNBIG=ALOG(250*NEQ)/ALOG(MAG)
730=      IF(RNBIG.LE.50.) GO TO 11

```

```

740= WRITE(8,998)
750= GO TO 777
760=11 WRITE(8,996)NRBIG
770=996 FORMAT(1X,*CALCULATED NBIG = *,G14.7,*INPUT INTEGER CHOICE:*,/)
780= READ *,NBIG
790= WRITE(8,979)NBIG
800= WRITE(8,993)
810=993 FORMAT(1X,*INPUT ZERO TO LIST EIGENVALUES :*,/)
820= READ *,MTEST1
830= WRITE(8,979)MTEST1
840=C*****
850=C
860=C COMPUTE COEFFICIENTS OF THE POLYNOMIAL
870=C  $F(Z) = \text{COEF}(1) * Z^{**\text{NDEG}} + \text{COEF}(2) * Z^{**(\text{NDEG}-1)} + \dots +$ 
880=C  $\text{COEF}(\text{NDEG}) * Z + \text{COEF}(\text{NDEG}+1)$ 
890=C
900=C*****
910= ALPHA=-1.+DELTA
920= BETA=1.+DELTA
930= COEF(1)=CMPLX(1.,0.)
940= NDEG=2*NRBIG+1
950= NCOEF=NDEG+1
960= M=NRBIG+1
970= DO 15 I=1,M
980= AN1=CSQRT(4.*EYE*PI*T/MSUBN(I))
990= AN2=-I*EYE/MSUBN(I)
1000= AN3=BETA*(1.-1./MSUPN(I+1))
1010= AN4=ALPHA*(1.-1./MSUPN(I+1))
1020= AN5=BETA-ALPHA/MSUPN(I+1)
1030= AN6=ALPHA-BETA/MSUPN(I+1)
1040= FBETA(I)=-(CEXP(AN2*AN3**2)/AN3)/AN1
1050= FALPHA(I)=-(CEXP(AN2*AN5**2)/AN5)/AN1
1060= GBETA(I)=(CEXP(AN2*AN6**2)/AN6)/AN1
1070= GALPHA(I)=(CEXP(AN2*AN4**2)/AN4)/AN1
1080=15 CONTINUE
1090= FALPHA(M)=CEXP(AN2*BETA**2)/BETA/(-AN1)
1100= FBETA(M)=FALPHA(M)
1110= GBETA(M)=CEXP(AN2*ALPHA**2)/ALPHA/AN1
1120= GALPHA(M)=GBETA(M)
1130= COEF(2)=-(FBETA(1)+GALPHA(1)+1.)
1140= L1=NRBIG+2
1150= NA=1
1160= NB=1
1170= DO 21 I=3,L1
1180= X2=CMPLX(0.,0.)
1190= Y2=X2
1200= DO 18 JA=1,NA
1210= KA=NA-JA+1
1220= X1=FBETA(JA)*GALPHA(KA)-FALPHA(JA)*GBETA(KA)
1230= X2=X1+X2
1240=18 CONTINUE
1250= IF(I.EQ.3) GO TO 20
1260= DO 19 JB=1,NB
1270= KB=NB-JB+1
1280= Y1=FALPHA(JB)*GBETA(KB)-FBETA(JB)*GALPHA(KB)
1290= Y2=Y1+Y2
1300=19 CONTINUE
1310= NB=NB+1
1320=20 Z1=FBETA(I-2)-FBETA(I-1)
1330= Z2=GALPHA(I-2)-GALPHA(I-1)
1340= COEF(I)=X2+Y2+Z1+Z2
1350= NA=NA+1
1360=21 CONTINUE
1370= L2=NRBIG+3

```

```

1380=      NA=NBIG-1
1390=      NB=NBIG-1
1400=      DO 28 I=L2, NCOEF
1410=      X2=CMPLX(0.,0.)
1420=      Y2=X2
1430=      IF(I.EQ.NCOEF) GO TO 23
1440=      DO 22 JA=1,NA
1450=      KA=NBIG+JA-NA
1460=      X1=FBETA(M-JA)*GALPHA(KA)-FALPHA(M-JA)*GBETA(KA)
1470=      X2=X1+X2
1480=22     CONTINUE
1490=      IF(I.EQ.L2) GO TO 25
1500=23     DO 24 JB=1,NB
1510=      KB=NBIG+JB-NB
1520=      Y1=FALPHA(M-JB)*GBETA(KB)-FBETA(M-JB)*GALPHA(KB)
1530=      Y2=Y1+Y2
1540=24     CONTINUE
1550=      NB=NB-1
1560=      GO TO 27
1570=25     DO 26 JB=1,NBIG
1580=      KB=NBIG-JB+1
1590=      Y1=FALPHA(JB)*GBETA(KB)-FBETA(JB)*GALPHA(KB)
1600=      Y2=Y1+Y2
1610=26     CONTINUE
1620=27     Z1=FBETA(M)*(GALPHA(I-M-1)-GBETA(I-M-1))
1630=      Z2=GALPHA(M)*(FALPHA(I-M-1)-FBETA(I-M-1))
1640=      COEF(I)=X2+Y2+Z1-Z2
1650=      NA=NA-1
1660=28     CONTINUE
1670=C*****
1680=C
1690=C      COMPUTE ROOTS OF POLYNOMIAL WITH IMSL ROUTINE ZCPOLY. TO
1700=C      OBTAIN THE EIGENVALUES. AND THEN ORDER EIGENVALUES BY
1710=C      SIZE.
1720=C
1730=C*****
1740=      CALL ZCPOLY(COEF,NDEG,LAMBDA,IER)
1750=      IF(MTEST1.EQ.0) WRITE(8,89)
1760=      I=1
1770=      DO 70 I1=2,NDEG
1780=      SIZE= REAL(LAMBDA(I))*2+AIMAG(LAMBDA(I))*2
1790=      K=I
1800=      DO 75 J=I1,NDEG
1810=      SIZE1=REAL(LAMBDA(J))*2+AIMAG(LAMBDA(J))*2
1820=      IF(SIZE1.LT.SIZE) GO TO 75
1830=      K=J
1840=      SIZE=SIZE1
1850=75     CONTINUE
1860=      CDUM=LAMBDA(I)
1870=      LAMBDA(I)=LAMBDA(K)
1880=      LAMBDA(K)=CDUM
1890=      CL(I)=LAMBDA(I)
1900=      EVPH=ATAN2(AIMAG(CL(I)),REAL(CL(I)))*180./PI
1910=      SMA=REAL(CL(I))*2+AIMAG(CL(I))*2
1920=      SMAG=SQRT(SMA)
1930=      IF(MTEST1.EQ.0) WRITE(8,333)I,LAMBDA(I),SMAG,EVPH
1940=333    FORMAT(1X,I9,1X,4(G14.7,1X),/)
1950=      I=I1
1960=70     CONTINUE
1970=      EVPH=ATAN2(AIMAG(LAMBDA(NDEG)),REAL(LAMBDA(NDEG)))*180./PI
1980=      SMA=REAL(LAMBDA(NDEG))*2+AIMAG(LAMBDA(NDEG))*2
1990=      SMAG=SQRT(SMA)
2000=      IF(MTEST1.EQ.0) WRITE(8,333)NDEG,LAMBDA(NDEG),SMAG,EVPH

```

```

2010=C*****
2020=C
2030=C      NOW CALCULATE THE CONSTANTS FOR THE FUNCTION SUM FOR A PAR-
2040=C      TICULAR MODE. THEN LOOP TO CALCULATE THE FIELD AT A SELECTED
2050=C      NUMBER OF POINTS.
2060=C
2070=C*****
2080=45      WRITE(8,997)
2090=997      FORMAT(1X,*INPUT 0 TO CONTINUE, 1 TO DO NEW CAVITY, OR 2 TO EXIT:*)
2100=      1 ,/)
2110=      READ *,MTEST2
2120=      WRITE(8,979)MTEST2
2130=      IF(MTEST2-1) 100,777,888
2140=100      WRITE(8,995)
2150=995      FORMAT(1X,*INPUT DESIRED MODE NUMBER:*,/)
2160=      READ *,MODE
2170=      WRITE(8,979)MODE
2180=      LABEL(15)=10H  MODE #
2190=      ENCODE(10,987,LABEL(16))MODE
2200=987      FORMAT(4X,I2,4X)
2210=      ROOT=LAMBDA(MODE)
2220=      WRITE(4)MODE,ROOT
2230=      X2=CMPLX(0.,0.)
2240=      Y2=X2
2250=      Z2=X2
2260=      DO 40 I=1,NBIG
2270=      RINDEX(I)=I
2280=      AN1=ROOT**-(NBIG-I)
2290=      X1=AN1*FALPHA(I)*(ROOT-1.)/FBETA(M)
2300=      X2=X1+X2
2310=      Y1=AN1*GALPHA(I)
2320=      Y2=Y1+Y2
2330=      Z1=AN1*FALPHA(I)*GBETA(M)/FBETA(M)
2340=      Z2=Z1+Z2
2350=40      CONTINUE
2360=      DO 41 I=1,NBIG
2370=      AN1=ROOT**-(NBIG-I)
2380=      CONSTB(I)=AN1*(X2+1.)/(ROOT**NBIG-Y2+Z2)
2390=      CONSTA(I)=(AN1*(ROOT-1.)-CONSTB(I)*GBETA(M))/FBETA(M)
2400=41      CONTINUE
2410=      WRITE(8,982)
2420=982      FORMAT(1X,*INPUT 0 TO CALC INTENSITY, 1 TO CONTINUE, OR 2 TO EXIT:*)
2430=      1 ,*)
2440=      READ *,MTEST3
2450=      WRITE(8,979)MTEST3
2460=      ENCODE(10,994,LABEL(2))NEQ
2470=      ENCODE(10,994,LABEL(4))MAG
2480=      ENCODE(10,990,LABEL(14))DELTA
2490=      ENCODE(10,980,LABEL(7))REAL(ROOT)
2500=      ENCODE(10,980,LABEL(8))AIMAG(ROOT)
2510=980      FORMAT(610,4)
2520=      IF(MTEST3-1) 101,102,888
2530=101      LABEL(9)=10HMIRROR
2540=      LABEL(10)=10HPLANE
2550=      LABEL(11)=10HSCALED
2560=      LABEL(12)=10H INTENSITY
2570=      LABEL(17)=10H PHASE
2580=      LABEL(18)=10H (DEG)
2590=      WRITE(8,222)
2600=222      FORMAT(1X,*INPUT 0 TO CALC INTENSITY OVER EXPANDED RANGE:*,/)
2610=      READ *,MTEST4
2620=      WRITE(8,979)MTEST4
2630=      IF(MTEST4.NE.0) GO TO 104

```

```

2640=      CALL ALLINT(MAG,MSURN,MSUPN,CONSTA,CONSR,T,NBIG,ROOT,
2650=      1 ALPHA,BETA,LABEL,DELTA,MODE)
2660=      GO TO 102
2670=104    WRITE(8,992)
2680=992    FORMAT(1X,*INPUT INCREMENT OF X FOR PLOT:*,/)
2690=      READ *,INCX
2700=      WRITE(8,979)INCX
2710=      WRITE(8,950)
2720=950    FORMAT(1X,*INPUT 0 TO LIST FIELD, PHASE, AND INTENSITY : *,/)
2730=      READ *,MTESTS
2740=      WRITE(8,979)MTESTS
2750=      IF(MTESTS.NE.0) GO TO 556
2760=      WRITE(8,554)
2770=554    FORMAT(17X,*FIELD*,20X,*INTENSITY*,11X,*X*,11X,*PHASE (DEG)*,/)
2780=556    NDATA=0
2790=      X=ALPHA
2800=      BRIGHT=0.
2810=31     NDATA=NDATA+1
2820=      STOREX(NDATA)=X
2830=      X1=CMPLX(0.,0.)
2840=      X2=X1
2850=      DO 32 I=1,NBIG
2860=      AN1=CSQRT(4.*EYE*PI*T/MSURN(I))
2870=      AN2=-T*EYE/MSURN(I)
2880=      AN3=ALPHA-X/MSURN(I+1)
2890=      AN4=BETA-X/MSURN(I+1)
2900=      FNX=-CONSTA(I)*CEXP(AN2*AN4**2)/AN1/AN4
2910=      GNX=-CONSTB(I)*CEXP(AN2*AN3**2)/AN1/AN3
2920=      X1=FNX+X1
2930=32     X2=GNX+X2
2940=      FIELD(NDATA)=1+X1+X2
2950=      XINTEN(NDATA)=REAL(FIELD(NDATA))**2+AIMAG(FIELD(NDATA))**2
2960=      PHASE(NDATA)=ATAN2(AIMAG(FIELD(NDATA)),REAL(FIELD(NDATA)))
2970=      PHASE(NDATA)=PHASE(NDATA)*180./PI
2980=      A1=-AIMAG(FIELD(NDATA))
2990=      A2=-REAL(FIELD(NDATA))
3000=      PHASE2(NDATA)=ATAN2(A1,A2)
3010=      PHASE2(NDATA)=PHASE2(NDATA)*180./PI
3020=      IF(XINTEN(NDATA).GT.BRIGHT) BRIGHT=XINTEN(NDATA)
3030=      IF(MTESTS.NE.0) GO TO 557
3040=      WRITE(8,555)FIELD(NDATA),XINTEN(NDATA),STOREX(NDATA),PHASE(NDATA)
3050=555    FORMAT(5X,2G14.7,5X,614.7,5X,614.7,5X,F7.2)
3060=557    X=X+1./INCX
3070=      IF(X.LE.BETA) GO TO 31
3080=      N1=NDATA+1
3090=      N2=0
3100=      PHASE(N1)=0.
3110=      DO 37 I=1,NDATA
3120=      THETA=ABS(PHASE(I+1)-PHASE(I))
3130=      IF(THETA.GT.300.) N2=N2+1
3140=37     XINTEN(I)=XINTEN(I)/BRIGHT
3150=      CALL HGRAPH(STOREX,XINTEN,NDATA,LABEL,1,0,0)
3160=      IF(N2.GT.1) GO TO 38
3170=      CALL HGRAPH(STOREX,PHASE,NDATA,LABEL,3,0,0)
3180=      GO TO 102
3190=38     CALL HGRAPH(STOREX,PHASE2,NDATA,LABEL,3,0,0)
3200=102    WRITE(8,991)
3210=991    FORMAT(1X,*TYPE 0 TO PLOT CONSIS VS N, 1 TO RETURN, OR 2 TO EXIT:
3220=      1 *,/)
3230=      READ *,MTEST6
3240=      WRITE(8,979)MTEST6
3250=      IF(MTEST6-1) 103,45,868
3260=103    LABEL(9)=10HCONSTANT *
3270=      LABEL(10)=10H

```

```

3280= LABEL(11)=10H MOD(CONST
3290= LABEL(12)=10HANT A)**2
3300= DO 42 I=1,NBIG
3310= PCONA(1)=REAL(CONST(1))**2+AIMAG(CONST(1))**2
3320=42 PCONR(1)=REAL(CONSTR(1))**2+AIMAG(CONSTR(1))**2
3330= CALL HGRAPH(RINDEX,PCONA,NBIG,LABEL,1,-1,11)
3340= LABEL(12)=10HANT B)**2
3350= CALL HGRAPH(RINDEX,PCONR,NBIG,LABEL,1,-1,11)
3360= WRITE(8,984)MODE
3370=984 FORMAT(1X,*COMPLETED PLOT OF CONSTANTS, MODE =*,12,/)
3380= GO TO 45
3390=978 FORMAT(1X,*INPUT VALUES ARE : *,2(5,/)
3400=979 FORMAT(1X,*INPUT VALUE IS : *,15,/)
3410=998 FORMAT(1X,*REVISE PARAMETERS SO NDEG < 24*)
3420=88 FORMAT(10X,*MAG = *,F6.3,5X,*NEP = *,F6.3,5X,*DELTA = *,
3430= 1 F6.5,/)
3440=89 FORMAT(9X,*I*,2X,*LAMBDA(REAL)*,3X,*LAMBDA(IMAG)*,6X,
3450= 1 *EVMAG*,10X,*EVPH*,/)
3460=888 CALL EXIT
3470= END
3480= SUBROUTINE ALLINT(MAG,MSURN,MSUPN,CONSTA,CONSTR,I,NBIG,ROOT,
3490= 1 ALPHA,BETA,LABEL,DELTA,MODE)
3500= DIMENSION LABEL(25),NCOUNT(10),J(25)
3510= COMMON STOREX(700),PHASE(700),XINTEN(700),PHASE2(700)
3520= REAL MSURN(51),MSUPN(51),INARG1,INARG2,INARG3,INARG4,INARG5
3530= REAL INARG6,INARG7,INARG8,MAG,MINV
3540= COMPLEX APART1,APART2,BPART1,BPART2,ALLFUN,CONSTA(51),ROOT,EYE
3550= COMPLEX AFUN,BFUN,SPNTU0,SPNTU1,UOY,OUTCON,FRESL,CONSTR(51)
3560= COMPLEX EYEFAC,EYEF1,EYEF2,SPNTU2,VAR4,FIELD(700)
3570=C*****
3580=C
3590=C THIS SUBROUTINE FOLLOWS PROGRAM BARC AND COMPUTES BEAM INTENSITIES
3600=C IN THE OUTPUT PLANE. 4 INTERMEDIATE POINTS FOR EVALUATION ARE INPUT
3610=C WHILE ALL OTHER REQUIRED QUANTITIES ARE CARRIED THROUGH IN THE
3620=C ARGUMENT LIST AS FOLLOWS:
3630=C
3640=C MAG= CAVITY MAGNIFICATION
3650=C MSURN= ARRAY FOR PARTIAL SUMS OF INVERSE POWERS OF MAG
3660=C MSUPN= ARRAY FOR MAG TO SOME POWER
3670=C CONST= ARRAY OF CONSTANTS IN THE ASYMPTOTIC SERIES
3680=C T= QUANTITY DEFINED IN BARC PER HORWITZ
3690=C NBIG= 4 TERMS IN THE SERIES
3700=C ROOT= MODE EIGENVALUE
3710=C LABEL= PLOT LABELING ARRAY
3720=C
3730=C*****
3740= NDATA=1
3750= BRIGHT=0.
3760= SX1=0.0
3770= SX2=0.0
3780= SY1=0.0
3790= SXY=0.0
3800= DO 5 I=1,10
3810=5 NCOUNT(I)=0
3820= X1=(-1.+DELTA)*MAG
3830= X2=(1.+DELTA)*MAG
3840= PI=2.*ASIN(1.)
3850= EYE=CMPLX(0.,1.)
3860= EYEFAC=(1.-EYE)/2.
3870= WRITE(8,900)
3880=900 FORMAT(1H1,*ENTERING EXTENDED RANGE INTENSITY SUBROUTINE.*,/)
3890= DO 10 I=1,51
3900=10 MSUPN(I)=MAG*MSUPN(I)
3910= WRITE(8,901)

```

```

3920=901   FORMAT(1X,*INPUT MIN AND MAX X VALUES AND # POINTS BETWEEN: *,/)
3930=      READ *,XMIN,XMAX,INCX
3940=      WRITE(8,902)XMIN,XMAX,INCX
3950=902   FORMAT(1X,*INPUT VALUES ARE : *,F5.2,2X,F5.2,2X,I5,/)
3960=903   FORMAT(1X,*INPUT VALUE IS : *,I5,/)
3970=      WRITE(8,904)
3980=904   FORMAT(1X,*INPUT 0 TO LIST FIELD, PHASE, AND INTENSITY : *,/)
3990=      READ *, NTEST1
4000=      WRITE(8,903) NTEST1
4010=      IF(NTEST1.NE.0) GO TO 20
4020=      WRITE(8,905)
4030=905   FORMAT(17X,*FIELD*,20X,*INTENSITY*,11X,*X*,11X,*PHASE (DEG)*,
4040=      1 11X,*PHASE2 (DEG)*,/)
4050=20    X=XMIN
4060=50    ALLFUN=(0.,0.)
4070=      DO 310 I=1,NRIG
4080=      MINV=1./MSUBN(I)
4090=      VAR1=2.*(1.+1./MSUBN(2*I)/MSUBN(I))
4100=      VAR2=SQRT(4.*T/P1/VAR1)
4110=      VAR3=MINV/MSUBN(I)
4120=      STAPHA=(X/MAG+I*ETA*VAR3)/(1.5*VAR1)
4130=      STAPHB=(X/MAG+ALPHA*VAR3)/(1.5*VAR1)
4140=      INARG1=(I*ETA-X/MAG)**2+(I*ETA-I*ETA*MINV)**2/MSUBN(I)
4150=      INARG2=(I*ETA-X/MAG-I*ETA*(1.-MINV)*VAR3)**2/(1.5*VAR1)
4160=      AARG1=INARG2-INARG1
4170=      APART1=CEXP(EYE*I*AARG1)*(-CONSTA(I))/(I*ETA-I*ETA*MINV)
4180=      INARG3=(ALPHA-X/MAG)**2+(I*ETA-ALPHA*MINV)**2/MSUBN(I)
4190=      INARG4=(ALPHA-X/MAG-(I*ETA-ALPHA*MINV)*VAR3)**2/(1.5*VAR1)
4200=      AARG2=INARG4-INARG3
4210=      APART2=CEXP(EYE*I*AARG2)*(-CONSTA(I))/(I*ETA-ALPHA*MINV)
4220=      INARG5=(I*ETA-X/MAG)**2+(ALPHA-I*ETA*MINV)**2/MSUBN(I)
4230=      INARG6=(I*ETA-X/MAG-(ALPHA-I*ETA*MINV)*VAR3)**2/(1.5*VAR1)
4240=      BARG1=INARG6-INARG5
4250=      BPART1=CEXP(BARG1*I*EYE*I)*CONSTB(I)/(ALPHA-I*ETA*MINV)
4260=      INARG7=(ALPHA-X/MAG)**2+(ALPHA-ALPHA*MINV)**2/MSUBN(I)
4270=      INARG8=(ALPHA-X/MAG-ALPHA*(1.-MINV)*VAR3)**2/(1.5*VAR1)
4280=      BARG2=INARG8-INARG7
4290=      BPART2=CEXP(BARG2*I*EYE*I)*CONSTB(I)/(ALPHA-ALPHA*MINV)
4300=      OUTCON=SQRT(MSUBN(I)/P1/T/VAR1)/2./ROOT
4310=      FRSA1=VAR2*(I*ETA-X/MAG-I*ETA*(1.-MINV)*VAR3)
4320=      FRSA2=VAR2*(ALPHA-X/MAG-(I*ETA-ALPHA*MINV)*VAR3)
4330=      FRSB1=VAR2*(I*ETA-X/MAG-(ALPHA-I*ETA*MINV)*VAR3)
4340=      FRSB2=VAR2*(ALPHA-X/MAG-ALPHA*(1.-MINV)*VAR3)
4350=      EYEF1=EYEFAC
4360=      EYEF2=EYEFAC
4370=      IF(STAPHA.GT.I*ETA) EYEF2=-EYEFAC
4380=      IF(STAPHB.GT.I*ETA) EYEF1=-EYEFAC
4390=      IF(STAPHA.GE.ALPHA.AND.STAPHB.LE.I*ETA) EYEF2=-EYEFAC
4400=      AFUN=APART1*(FRESL(FRSA1)-EYEF1)-APART2*(FRESL(FRSA2)-EYEF2)
4410=      SPNTU1=CEXP(-EYE*(P1/4.+T*((STAPHA-X/MAG)**2+(I*ETA-
4420=      1  STAPHA*MINV)**2/MSUBN(I))))/(I*ETA-STAPHA*MINV)*(-CONSTA(I))
4430=      IF(STAPHA.GE.ALPHA.AND.STAPHB.LE.I*ETA) AFUN=AFUN+SPNTU1*SQRT(2.)
4440=      EYEF1=EYEFAC
4450=      EYEF2=EYEFAC
4460=      IF(STAPHB.GT.I*ETA) EYEF1=-EYEFAC
4470=      IF(STAPHB.GT.I*ETA) EYEF2=-EYEFAC
4480=      IF(STAPHB.GE.ALPHA.AND.STAPHA.LE.I*ETA) EYEF2=-EYEFAC
4490=      BFUN=BPART1*(FRESL(FRSB1)-EYEF1)-BPART2*(FRESL(FRSB2)-EYEF2)
4500=      SPNTU2=CEXP(-EYE*(P1/4.+T*((STAPHB-X/MAG)**2+(ALPHA-STAPHB*
4510=      1  MINV)**2/MSUBN(I))))/(ALPHA-STAPHB*MINV)*CONSTB(I)
4520=      IF(STAPHB.GE.ALPHA.AND.STAPHA.LE.I*ETA) BFUN=BFUN+SPNTU2*SQRT(2.)
4530=      ALLFUN=OUTCON*(AFUN+BFUN)+ALLFUN
4540=310   CONTINUE
4550=      EYEF1=EYEFAC

```



```

4560=      EYEF2=EYEFAC
4570=      IF(X/MAG.GT.BETA) EYEF1=-EYEFAC
4580=      IF(X/MAG.GT.BETA) EYEF2=-EYEFAC
4590=      IF(X/MAG.GE.ALPHA.AND.X/MAG.LE.BETA) EYEF2=-EYEFAC
4600=      FRSU01=SQRT(2.*T/PI)*(BETA-X/MAG)
4610=      FRSU02=SQRT(2.*T/PI)*(ALPHA-X/MAG)
4620=      VAR4=CSQRT(EYE/2.)/ROOT
4630=      UOX=VAR4*((FRESL(FRSU01)-EYEF1)-(FRESL(FRSU02)-EYEF2))
4640=      SPNTU0=DEXP(-EYE*PI/4.)*VAR4*SQRT(2.)
4650=      IF(X/MAG.GE.ALPHA.AND.X/MAG.LE.BETA) UOX=UOX+SPNTU0
4660=      ALLFUN=ALLFUN+UOX
4670=      FIELD(NDATA)=ALLFUN
4680=      STOREX(NDATA)=X
4690=      XINTEN(NDATA)=AIMAG(ALLFUN)**2+REAL(ALLFUN)**2
4700=      PHASE(NDATA)=ATAN2(AIMAG(ALLFUN),REAL(ALLFUN))
4710=      PHASE(NDATA)=PHASE(NDATA)*180./PI
4720=      PHASE2(NDATA)=ATAN2(-AIMAG(ALLFUN),-REAL(ALLFUN))
4730=      PHASE2(NDATA)=PHASE2(NDATA)*180./PI
4740=      IF(XINTEN(NDATA).GT.BRIGHT) BRIGHT=XINTEN(NDATA)
4750=      IF(NTEST1.NE.0) GO TO 400
4760=      WRITE(8,906)ALLFUN,XINTEN(NDATA),STOREX(NDATA),PHASE(NDATA),
4770=      1 PHASE2(NDATA)
4780=906  FORMAT(5X,2G14.7,5X,614.7,5X,614.7,5X,F7.2,15X,F7.2)
4790=400  X=X+1./INCX
4800=      IF(X.GT.XMAX) GO TO 500
4810=      NDATA=NDATA+1
4820=      GO TO 50
4830=500  N1=NDATA+1
4840=      PHASE(N1)=0.
4850=      DO 510 I=1,NDATA
4860=      IF(STOREX(I).LE.X1) J(24)=I+1
4870=      IF(STOREX(I).LE.X2) J(25)=I+1
4880=510  XINTEN(I)=XINTEN(I)/BRIGHT
4890=      K=0
4900=      J1=J(24)
4910=      J2=J(25)
4920=      DO 520 I=J1,J2
4930=      THETA2=ABS(PHASE2(I+1)-PHASE2(I))
4940=      THETA=ABS(PHASE(I+1)-PHASE(I))
4950=      IF(THETA2.GT.300.) NCOUNT(2)=NCOUNT(2)+1
4960=      IF(THETA.LE.300.) GO TO 520
4970=      K=K+1
4980=      J(K)=I
4990=      NCOUNT(1)=NCOUNT(1)+1
5000=520  CONTINUE
5010=      DO 530 I=1,51
5020=530  MSUPN(I)=MSUPN(I)/MAG
5030=      WRITE(8,907)
5040=907  FORMAT(1X,*INPUT 0 TO PLOT INTENSITY AND PHASE : */)
5050=      READ *,NTEST2
5060=      WRITE(8,903) NTEST2
5070=      IF(NTEST2.NE.0) GO TO 550
5080=      CALL HGRAPH(STOREX,XINTEN,NDATA,LABEL,1,0,0)
5090=      IF(NCOUNT(1).GT.1) GO TO 535
5100=      CALL HGRAPH(STOREX,PHASE,NDATA,LABEL,3,0,0)
5110=      GO TO 550
5120=535  CONTINUE
5130=      IF(NCOUNT(2).GT.1) GO TO 537
5140=      CALL HGRAPH(STOREX,PHASE2,NDATA,LABEL,3,0,0)
5150=      GO TO 550
5160=537  K=1
5170=540  J1=J(K)
5180=      J2=J(K+1)-1
5190=      IF(K.EQ.NCOUNT(1)) J2=J(25)

```

```

5200=      DO 545 I=J1,J2
5210=      IF(PHASE(J1).GT.0.0) PHASE(I+1)=PHASE(I+1)+360.
5220=      IF(PHASE(J1).LT.0.0) PHASE(I+1)=PHASE(I+1)-360.
5230=545   CONTINUE
5240=      K=K+2
5250=      IF(K.LE.NCOUNT(1)) GO TO 540
5260=      CALL HGRAPH(STOREX,PHASE,NDATA,LABEL,3,0,0)
5270=550   J1=J(24)
5280=      J2=J(25)
5290=      IF(MODE.NE.1) GO TO 565
5300=      DO 563 I=J1,J2
5310=      PHASE=PHASE(I)*PI/180.
5320=      SX1=SX1+STOREX(I)
5330=      SX2=SX2+STOREX(I)**2
5340=      SY1=SY1+PHASE
5350=      SXY=SXY+STOREX(I)*PHASE
5360=563   NCOUNT(3)=NCOUNT(3)+1
5370=      SLOPE=ABS((SY1*SX1-SXY*NCOUNT(3))/(SX1**2-SX2*NCOUNT(3)))
5380=      WRITE(8,910)SLOPE
5390=910   FORMAT(1X,* SLOPE = *,G14.7,/)
5400=565   WRITE(4)NDATA,1./INCX
5410=      DO 580 I=1,NDATA
5420=580   WRITE(4)FIELD(I),STOREX(I+INCX)
5430=      WRITE(8,920)
5440=920   FORMAT(1X,*COMPLETED CALCULATION AND PLOT, EXTENDED.*,/)
5450=      RETURN
5460=      END
5470=C*****
5480=      SUBROUTINE HGRAPH(X,Y,N,ID,NO,NP,NS)
5490=      DIMENSION X(1),Y(1),ID(25) $ IF (NO.EQ.2) CALL PLOT(-1.05,2.10,-3)
5500=      IF (NO.EQ.2) GO TO 30 $ IF (NO.LT.0) GO TO 10
5510=      CALL SCALE(X,7.,N,1) $ CALL SCALE(Y,5.,N,1)
5520=10     CALL PLOT(0.,11.,2) $ CALL PLOT(8.5,11.,2)
5530=      CALL PLOT(8.5,0.,2) $ CALL PLOT(0.,0.,2)
5540=      CALL PLOT(1.35,1.35,-3) $ CALL PLOT(0.,8.30,-2)
5550=      IF(ID(1).EQ.999) GO TO 25
5560=      CALL PLOT(.1,-.1,-3) $ CALL PLOT(0.,-2.,-2)
5570=      CALL SYMBOL(.25,.3,.07,ID(1),90.,20)
5580=      CALL SYMBOL(.45,.3,.07,ID(3),90.,20)
5590=      CALL SYMBOL(.65,.3,.07,ID(13),90.,20)
5600=      CALL SYMBOL(.85,.3,.07,ID(15),90.,20)
5610=      CALL SYMBOL(1.05,.3,.07,ID(5),90.,20)
5620=      CALL SYMBOL(1.15,.3,.07,ID(7),90.,20)
5630=      CALL PLOT(0.,0.,3) $ CALL PLOT(1.25,0.,2)
5640=      CALL PLOT(1.25,2.,2) $ CALL PLOT(0.,2.,-2)
5650=      CALL PLOT(-.1,.1,-3)
5660=25     CALL PLOT(5.8,0.,-2)
5670=      CALL PLOT(0.,-8.30,-2) $ CALL PLOT(-5.8,0.,-2)
5680=      CALL PLOT(5.3,.75,-3)
5690=      CALL AXIS(0.,0.,ID(9),-20,7.,90.,X(N+1),X(N+2))
5700=      IF(NO.EQ.3) GO TO 27
5710=      CALL AXIS(0.,0.,ID(11),20,5.,180.,Y(N+1),Y(N+2))
5720=      GO TO 30
5730=27     CALL AXIS(0.,0.,ID(17),20,5.,180.,Y(N+1),Y(N+2))
5740=30     Y(N+2)=-Y(N+2) $ CALL LINE(Y,X,N,1,NP,NS)
5750=      Y(N+2)=-Y(N+2) $ CALL PLOT(1.85,-2.10,-3)
5760=      RETURN $ END
5770=      SUBROUTINE AXIS(X0,Y0,L,NC,RL,ANG,RMIN,DR)
5780=      DIMENSION L(1) $ A=ANG*3.14159/180. $ DX=.1*COS(A) $ DY=.1*SIN(A)
5790=      IC=ISIGN(1,NC) $ NNC=IABS(NC) $ R=.1 $ N=1 $ X=X0 $ Y=Y0
5800=10     CALL PLOT(X,Y,3) $ X=X+DX $ Y=Y+DY $ CALL PLOT(X,Y,2)
5810=      CALL PLOT(X-.21*DY*IC,Y+.21*DX*IC,2)
5820=      IF(N.EQ.5) CALL PLOT(X-.42*DY*IC,Y+.42*DX*IC,2)
5830=      IF(N.EQ.10) CALL PLOT(X-.70*DY*IC,Y+.70*DX*IC,2)

```

```

5840=      N=MOD(N,10)+1 2 R=R+.1 $ IF(R.LT.RL) GO TO 10
5850=      A=ANG-(IC+1)*45. $ IX=10.*IX $ IY=10.*IY
5860=      C=-.175+.125*IC      $      D=.19+.35*IC
5870=      X=X0+C*IX-I*NY      $      Y=Y0+C*IY+D*IX
5880=      R=AMAX1(ABS(RMIN),ABS(RMIN+DR*RL)) $ R=ALOG10(R)
5890=      IR=INT(ABS(R)) $ IF(R.LT.0.) IR=-(IR+1) $ IR=IR-MOD(IR,3)
5900=      R1=RMIN/10.**IR $ IR1=IR/10.**IR $ R=0.
5910=20    ENCODE(7,101,S)R1 $ CALL SYMBOL(X,Y,.07,S,A,7) $ R1=R1/IR1
5920=      X=X+IX $ Y=Y+IY $ R=R+1. $ IF(R.LE.RL) GO TO 20
5930=      R=(RL-.1*NNC)/2.      $      C=.14.5*IC
5940=      X=X0+R*IX-C*IY      $      Y=Y0+R*IY+C*IX
5950=      CALL SYMBOL(X,Y,.1,L,ANG,NNC) $ IF(IR.EQ.0) RETURN
5960=      ENCODE(5,102,S) $ CALL SYMBOL(999.,999.,.10,S,ANG,5)
5970=      CALL WHERE(X,Y,A)
5980=      ENCODE(3,103,S) IR $ CALL SYMBOL(X,Y,.07,S,ANG,3)
5990=101    FORMAT(F7.2)
6000=102    FORMAT(5H *10)
6010=103    FORMAT(I3)
6020=      RETURN $      END
6030=C*****
6040=C
6050=C      SUBROUTINE SCALE(DATA,LENGTH,N,K)
6060=C
6070=C      REAL DATA = N+2 DIMENSIONED AR. Y OF DATA TO BE SCALED
6080=C      INTEGER N = NUMBER OF DATA POINTS
6090=C      REAL LENGTH = LENGTH OF THE PLOT AXIS (E.G. IN INCHES)
6100=C      INTEGER K = UNUSED PARAMETER INCLUDED FOR COMPATIBILITY
6110=C      WITH THE EQUIVALENT CALCOMP SUBROUTINE
6120=C
6130=C      THE FOLLOWING VALUES ARE RETURNED:
6140=C
6150=C      DATA(N+1) = ADJUSTED DATA MINIMUM
6160=C      DATA(N+2) = "NICE" SCALE FACTOR IN DATA UNITS
6170=C      PER LENGTH UNIT (E.G. VOLTS/INCH)
6180=C
6190=C*****
6200=      SUBROUTINE SCALE(DATA,LENGTH,N,K)
6210=      REAL DATA(N), LENGTH, SF(5)
6220=      DATA SF /1., 2., 2.5, 5., 10. /
6230=
6240=C      COMPUTE THE RAW SCALE FACTOR
6250=
6260=      IMIN=IMAX=DATA(1)
6270=      DO 10 I=1,N
6280=          IF(DATA(I).LT. IMIN) IMIN = DATA(I)
6290=          IF (DATA(I).GT. IMAX) IMAX = DATA(I)
6300=10    CONTINUE
6310=C
6320=C      EXCLUDE TRIVIAL ERROR CASES
6330=C
6340=      DATA(N+1) = IMIN
6350=      DATA(N+2) = 1.0
6360=      IF (LENGTH .LE. 0.0 .OR. IMAX .EQ. IMIN ) RETURN
6370=      RAWSF = (IMAX - IMIN) / LENGTH
6380=
6390=C      RAWSF = SFMANT * 10. ** SFEXP, WHERE 1 .LE. SFMANT .LT. 10
6400=
6410=      SFEXP = AINT( ALOG10( RAWSF ) )
6420=      IF ( RAWSF .LT. 1.0 ) SFEXP = SFEXP - 1.0
6430=      SFMANT = RAWSF * 10.0 ** (-SFEXP)
6440=
6450=C      LOCATE NEXT LARGER "NICE" SCALE FACTOR
6460=
6470=      DO 20 I=1,5

```

```

6480=20      IF ( SF(I) .GT. SFMANT ) GO TO 30
6490=        PRINT*, " SCALE: SCALE FACTOR ERROR ... " $ RETURN
6500=30      SFNICE = SF(I) * 10.0 ** SFEXP
6510=
6520=C       COMPUTE ADJUSTED DATA MINIMUM
6530=
6540=        ADJMIN = AINT ( DMIN / SFNICE ) * SFNICE
6550=        IF ( ADJMIN .GT. RMIN ) ADJMIN = ARJMIN - SFNICE
6560=        IF ( (DMAX - ADJMIN) / SFNICE .LE. LENGTH ) GO TO 40
6570=
6580=C       NEED TO USE THE NEXT LARGER SCALE FACTOR
6590=
6600=        IF ( I .LT. 5 ) SFNICE = SF(I+1) * 10.0 ** SFEXP
6610=        IF ( I .EQ. 5 ) SFNICE = 20.0 * 10.0 ** SFEXP
6620=        ADJMIN = AINT ( DMIN / SFNICE ) * SFNICE
6630=        IF ( ARJMIN .GT. DMIN ) ARJMIN = ARJMIN - SFNICE
6640=40      CONTINUE
6650=        DATA(N+1) = ARJMIN
6660=        DATA(N+2) = SFNICE
6670=        RETURN
6680=        END
6690=C*****
6700=        COMPLEX FUNCTION CERF(ZZ)
6710=        COMPLEX ZZ,Z,A,A1,A2,R,B1,B2,F,F1
6720=        Z=ZZ
6730=        IF (CABS(Z) .GE. 3.) GO TO 30
6740=        J=0.
6750=        A=Z
6760=        R=Z
6770=        10 J=J+1
6780=        R=-Z*Z*CMPLX(FLOAT(2*J-1),0.)*R
6790=        R=R/CMPLX(FLOAT(J),0.)/CMPLX(FLOAT(2*J+1),0.)
6800=        A=A+R
6810=        IF (J .GE. 1000) GO TO 50
6820=        IF (CABS(R/A) .GE. (1.E-10)) GO TO 10
6830=        CERF=(1.128379167,0.)*A
6840=        RETURN
6850=        30 IF (REAL(ZZ) .LT. 0.) Z=-ZZ
6860=        A2=(1.,0.)
6870=        R2=Z
6880=        F2=A2/R2
6890=        A1=Z
6900=        B1=Z*Z*(0.5,0.)
6910=        F1=A1/B1
6920=        J=1
6930=        40 J=J+1
6940=        A=Z*A1+CMPLX(FLOAT(J)/2.,0.)*A2
6950=        B=Z*B1+CMPLX(FLOAT(J)/2.,0.)*B2
6960=        F=A/R
6970=        IF (J .GT. 1000) GO TO 50
6980=        IF (CABS((F-F1)/F) .LT. (1.E-10)) GO TO 60
6990=        A2=A1
7000=        B2=B1
7010=        A1=A
7020=        B1=B
7030=        F1=F
7040=        GO TO 40
7050=        50 WRITE (R,99)
7060=        99 FORMAT( " ERROR FUNCTION ROUTINE DID NOT CONVERGE ")
7070=        IER=1
7080=        RETURN
7090=        40 F1=(0.5,0.)*CEXP(-Z*Z)*F
7100=        CERF=1.128379167*F1
7110=        CERF=1.-CERF

```

```

7120=      IF (REAL(ZZ).LT.0.) CERF=-CERF
7130=      70 RETURN
7140=      END
7150=C*****
7160=      COMPLEX FUNCTION FRESL(X)
7170=      COMPLEX EYE,Z,CERF
7180=      EYE=(0.+1.) $ F1=2.*ASIN(1.)
7190=      Z=SQRT(F1)*X*(1.-EYE)/2.
7200=      FRESL=(1.+EYE)/2.*CERF(Z)
7210=      FRESL=CONJG(FRESL)
7220=      RETURN $ END

```

VITA

Richard W. Berdine, son of James E. and Betty R. Berdine, was born the 8th of April 1952 in Creston, Iowa. He graduated from East Union High School in Afton, Iowa on 25 May 1970. He then attended Iowa State University from September 1970 until May 1975 when he graduated with a B.S. degree in Engineering Science. After 2½ years in private industry he attended Officers Training School and was commissioned on 29 June 1978. His first assignment was to Aeronautical Systems Division, and after two years was reassigned to the Air Force Institute of Technology at Wright-Patterson AFB, Ohio.

Permanent Address: P.O. Box 5
Afton, Iowa 50830

REPORT DOCUMENTATION PAGE		READ INSTRUCTIONS BEFORE COMPLETING FORM
1. REPORT NUMBER AFIT/GEP/PH/81D-2	2. GOVT ACCESSION NO. AD-A118041	3. RECIPIENT'S CATALOG NUMBER
4. TITLE (and Subtitle) MODE ANALYSIS IN A MISALIGNED UNSTABLE RESONATOR		5. TYPE OF REPORT & PERIOD COVERED MS Thesis
		6. PERFORMING ORG. REPORT NUMBER
7. AUTHOR(s) Richard W. Berdine 1Lt USAF		8. CONTRACT OR GRANT NUMBER(s)
9. PERFORMING ORGANIZATION NAME AND ADDRESS Air Force Institute of Technology (AFIT/EN) Wright-Patterson AFB, Ohio 45433		10. PROGRAM ELEMENT, PROJECT, TASK AREA & WORK UNIT NUMBERS
11. CONTROLLING OFFICE NAME AND ADDRESS Air Force Institute of Technology (AFIT/EN) Physics Dept. Wright-Patterson AFB, Ohio 45433		12. REPORT DATE 18 December 1981
		13. NUMBER OF PAGES 83
14. MONITORING AGENCY NAME & ADDRESS (if different from Controlling Office) Air Force Institute of Technology (AFIT/EN) Physics Dept. Wright-Patterson AFB, Ohio 45433		15. SECURITY CLASS. (of this report) UNCLASSIFIED
		15a. DECLASSIFICATION/DOWNGRADING SCHEDULE
16. DISTRIBUTION STATEMENT (of this Report) Approved for public release; distribution unlimited.		
17. DISTRIBUTION STATEMENT (of the abstract entered in Block 20, if different from Report)		
18. SUPPLEMENTARY NOTES <div style="display: flex; justify-content: space-between;"> <div> <p><i>John E. Wolaver</i> LYNN E. WOLAVER Dean for Research and Professional Development</p> </div> <div> <p>Approved for public release; IAW AFR 190-17 Frederick C. Lynch, Major, USAF Director of Public Affairs AIR FORCE INSTITUTE OF TECHNOLOGY (ATC) WRIGHT-PATTERSON AFB, OH 45433</p> </div> <div> <p>23 JUL 1982</p> </div> </div>		
19. KEY WORDS (Continue on reverse side if necessary and identify by block number) Misaligned Resonator Unstable Resonator Tilted Reflectors Beam Steering Mode Analysis		
20. ABSTRACT (Continue on reverse side if necessary and identify by block number) The integral equation that describes mode structure of an unstable resonator with rectangular apertures is developed from scalar diffraction theory. This equation, modified to account for misalignments, is solved by applying the asymptotic methods developed by Horwitz. A second order approximation of the method of stationary phase is the employed to calculate phase and intensity values for all points in the output plane. The phase front is also curve fitted to a straight line over the geomet-		

UNCLASSIFIED

SECURITY CLASSIFICATION OF THIS PAGE (When Data Entered)

rical region for the lowest loss mode. From the slope of the straight line, a direction of propagation can be attributed to the wave. This is a diffracted beam steering angle and is additional to the geometric steering angle (i.e., the beam steering angle due to the geometric misalignment of either or both mirrors).

Plots of intensity and phase for various degrees of misalignments are presented as results of a computer program that utilizes the derived expressions. Also included are graphs of the phase slope versus mirror misalignment.

A

UNCLASSIFIED

SECURITY CLASSIFICATION OF THIS PAGE (When Data Entered)

FILMED
9-8